Buckling of Bulk Structures With Finite Prebuckling Deformation

Hongyu Zhao
State Key Laboratory of Nonlinear Mechanics,
Institute of Mechanics,
Chinese Academy of Sciences,
Beijing 100190, China;
School of Engineering Science,
University of Chinese Academy of Sciences,
Beijing 100049, China
e-mail: xiaodouzhao@163.com

Yewang Su[1]
State Key Laboratory of Nonlinear Mechanics,
Institute of Mechanics,
Chinese Academy of Sciences,
Beijing 100190, China;
School of Engineering Science,
University of Chinese Academy of Sciences,
Beijing 100049, China;
State Key Laboratory of Structural Analysis for Industrial Equipment,
Department of Engineering Mechanics,
Dalian University of Technology,
Dalian 116024, China
e-mail: yewangsu@imech.ac.cn

The prebuckling deformation of structures is neglected in most of the conventional buckling theory (CBT) and numerical method (CNM), because it is usually very small in conventional concepts. In the preceding paper (Su et al., 2019), we found a class of structures from the emerging field of stretchable electronics, of which the prebuckling deformation became large and essential for determining the critical buckling load, and developed a systematic buckling theory for 3D beams considering the effects of finite prebuckling deformation (FPD). For bulk structures that appear vastly in the advanced structures, a few buckling theories consider the effects of the prebuckling deformation in constitutive equations by energy method, which are significantly important but not straightforward and universal enough. In this paper, a systematic and straightforward theory for the FPD buckling of bulk structures is developed with the use of two constitutive models. The variables for the prebuckling deformation serve as the coefficients of the incremental displacements, deformation components, and stress in the buckling analysis. Four methods, including the CBT, CNM, DLU (disturbing-loading-unloading method) method and FPD buckling theory, are applied to the classic problems, including buckling of an elastic semi-plane solid and buckling of an elastic rectangular solid, respectively. Compared with the accurate buckling load from the DLU method, the FPD buckling theory is able to give a good prediction, while the CBT and CNM may yield unacceptable results (with 70% error for the buckling of an elastic semi-plane solid). [DOI: 10.1115/1.4053726]

Keywords: buckling, finite deformation mechanics, stretchable electronics, an elastic semi-plane solid, an elastic rectangular solid

1 Introduction

Euler and Lagrange raised the concept of buckling and established the pioneering mechanical theory for buckling analysis in the 18th and 19th centuries [1,2]. It plays an important role in both of the conventional civil and mechanical engineering, and the emerging nano and micro science and technology [3–8]. The buckling theory was prosperously developed in the past hundred years, focusing on beams, plates, shells and bulks, which dominate the structure designs of the civil and mechanical engineering [7]. Structures usually undergo four regimes during the bucking process: (1) the original regime without any load; (2) the onset of buckling subject to the critical buckling load, with the prebuckling deformation and the prebuckling stress/force before the bifurcation; (3) the buckling regime subject to the critical buckling load after the bifurcation; and (4) the postbuckling regime subject to the increasing/decreasing load. In the conventional structures, however, the prebuckling deformation is usually very small and is neglected in most of the conventional buckling theory (CBT) and numerical method (CNM), while the prebuckling force or stress in the second regime serves as the coefficients of the incremental displacements, deformation components, and stress. A few buckling theories consider the effects of the prebuckling deformation in constitutive equations by energy method [9–11], which are significantly important but not straightforward and universal enough.

In recent decades, soft materials, flexible, and stretchable structures spring up like mushrooms in the fields of soft robots and flexible electronics. For some of these structures, the prebuckling deformation is found to be large and becomes essential and indispensable in the buckling analysis [12,13]. In our preceding paper [13], we found a class of beam structures from the emerging field of stretchable electronics, of which the prebuckling deformation is large and essential for determining the critical buckling load. They are called the buckling problems with finite prebuckling deformation (FPD) buckling. Experiments, numerical simulation, and theoretical analysis were conducted to show the importance of prebuckling deformation on buckling analysis. A systematic and straightforward theory (FPD buckling theory) was developed to analyze the FPD buckling behaviors of beams and was applied to three classic problems, including lateral buckling of a three-point-bending beam, lateral buckling of a pure bending beam, and Euler buckling. Our FPD buckling theory for beams was able to give a good prediction, while the CBT (by Timoshenko et al.) and CNM (by commercial program packages) yielded unacceptable results (with 70% error for a three-point-bending beam with $h/b = 0.8$, for example).

The preceding paper [13] focused on the FPD buckling behaviors of straight beams that deformed in the three-dimensional space. Besides that, FPD buckling exists in many more structures, such as the buckling of semi-plane problem, the buckling of helical springs, lateral buckling of thick arches, buckling of thin-wall structures, etc. On the buckling of bulk structures, Biot started the early work with a mechanical theory of incremental deformation [14–17]. The theory focuses on the influence of prebuckling force or stress on incremental stress. The effects of the rotation are considered in the stress transformation and the buckling analysis. The theory is also extended to the structures with incompressible materials [16] and viscoelastic materials [15]. However, the effects of the prebuckling deformation are not considered in the theory. Based on the foundations of the nonlinear theory of elasticity [18], Kerr and Tang [19] Brunelle [20] investigated the stability of the elastic rectangular solid and the elastic semi-plane solid with the consideration of the prebuckling stress, but without that of the prebuckling deformation, respectively. Triatanfyllidis [21,23], Jiménez and Triantafyllidis

[1]Corresponding author.

Contributed by the Applied Mechanics Division of ASME for publication in the Journal of Applied Mechanics. Manuscript received November 8, 2021; final manuscript received January 28, 2022; published online February 15, 2022. Assoc. Editor: Pedro Reis.

[22], and Lee et al. [24] studied the buckling problems of various structures, including the semi-space solids, honeycombs, tubes, etc., with electro-mechanical material, magneto-mechanical material, elasto-plastic material, elasto-viscoplastic material, etc. However, the prebuckling deformation was always neglected in the buckling analysis of these models, because it is very small in these practical situations. For the first time, Chadwick and Ogden [11], Ogden and Fu [25], and Ogden [26] considered the effects of both the prebuckling stress and deformation by energy method. The energy of prebuckling deformation in the second regime of the clarified buckling process in the first paragraph takes effects in constitutive equations of the buckling analysis from second to third regime, which, to be specific, appears in the first-, second-, and third-order tensors of instantaneous elastic moduli. Based on this theory, Fu and Ogden [9], Fu and Rogerson [10], and Ogden and Fu [25] investigated the buckling of thick elastic bodies subjected to finite elastic deformations. However, the works of Fu and Ogden require a holonomic constitutive model rather than arbitrary one and adopt the first Piola-Kirchhoff stress to avoid the explicit effects of prebuckling deformation on the equilibrium equations. It is significant to carry out further theoretical investigation that is more universal and straightforward for arbitrary buckling analysis considering effects of the prebuckling deformation. Besides, various definitions of incremental stress [18,27–29] have been proposed considering the effects of prebuckling stress, which, in a sense, perplex the buckling analysis.

Recently, compressive buckling of the stiff film that is bonded on a prestrained compliant substrate, into a wrinkling mode has become a desirable means to generate micrometer-scale surface patterns for a wide range of applications in flexible electronics. Vast theoretical works have been devoted to the buckling analysis of these film-substrate structures. In the pioneering work by Khang et al. [8], Huang et al. [30], Huang [31], Chen and Hutchinson [32], and Bowden et al. [33], the stiff film and the compliant substrate are modeled as an elastic thin plate satisfying the nonlinear von Karman plate equations and linear elastic support, respectively, which gives a constant wavelength of the buckled film. The measurements show, however, a qualitative behavior characterized by a clear and systematic decrease in wavelength with increasing prestrain, contrary to the prediction of the theory [5,8]. To solve this question, a buckling theory [5,34] that accounts for finite geometry change of the substrate and the thin film is established to yield an accurate solution. In this theory, the bending energy and the membrane energy of the film are integrated over the length of strain-free thin film instead of the length of the buckled film/substrate system in the previous models. The analytical solution shows the prestrain-dependent buckling wavelength and agrees well with the experiments. Besides, a nonlinear buckling model is presented by Jiang et al. [35] for the buckling of thin films with finite width on compliant substrates. Analytical solution shows that the buckling amplitude and wavelength increase with the film width, which agrees well with experiments. In all above theories, the buckling analysis is only applied to the stiff film, while the compliant substrate is modeled as an elastic support. An alternative way is to apply the buckling analysis to the entire structure including both the stiff film and the compliant substrate. In this theoretical framework, the effects of prebuckling deformation should be considered, because the compliant substrate is usually subjected to a finite prestrain when entire film-substrate structure undergoes the critical buckling process (second to third regime).

On the other hand, as applications of soft materials, such as elastomers and gels, grow, there is increasing interest in the buckling of soft films on compliant substrates [36–40]. The buckling of soft films sensitively depends on the thickness and compressibility of the compliant substrates, the mechanical properties of the films as well as the sliding interface condition between the thin film and the compliant substrate. Specifically, Holland et al. [39] examines the buckling of soft films on compliant substrates, in which compressive strains arise in both films and substrate layers when compression is applied to the sides of the entire domain of the film/substrate system. The analytical model gives the Euler-Lagrange equations and the boundary conditions expressed in terms of the displacement component. The effects of the prebuckling deformations of soft films and compliant substrates in a simple mode are considered in the energetic analysis. The energy of prebuckling deformation in the second regime of the clarified buckling process in the first paragraph are considered in the total energy during the buckling analysis. However, the theory is restricted to the incompressible materials modeled by a strain-energy function and avoids the explicit effects of prebuckling deformation on the equilibrium equations and geometrical equations.

The finite element method, which includes the linear buckling method and the nonlinear bucking method, has been used in a variety of buckling analysis. The linear buckling method is based on the CBT, with the consideration of the prebuckling stress/force but without considering prebuckling deformation. It results in a linear eigenvalue problem in mathematics. The numerical solver for critical buckling loads and buckling modes of structures is *general/linear perturbation* in commercial program package ABAQUS (Dassault-Systèmes, 2010). It is effective to solve the problem of critical buckling for most of the existing structures with neglectable prebuckling deformation. Nonlinear analysis is powerful to accurately capture the mechanical behavior of structures with the consideration of the past history of both stress and deformation. However, in the nonlinear buckling method, the defect or disturbance must be imported to lead the structure to the buckling deformation mode, if the symmetricity hinders the bifurcation of the structure. Using the nonlinear buckling method, Wang et al. [41] and Bertoldi et al. [42,43] studied the buckling of the carefully designed materials with meso-structures that leads to novel effective behavior at the macroscale. Therefore, the existing numerical solvers are still not enough to analyze the buckling problems with effects of the prebuckling deformation straightforwardly, if the defects or disturbance are prohibited to apply.

In the present paper, we focus on the FPD buckling behaviors of bulk structures. A systematic and straightforward theory for the FPD buckling of bulk structures is developed in Sec. 2. Different types of constitutive models significantly affect the critical buckling load. Here, two constitutive models including the Saint-Venant-Kirchhoff model, which is $\boldsymbol{T}=\boldsymbol{L}:\boldsymbol{E}$ and $\overset{\nabla}{\boldsymbol{\tau}}=\boldsymbol{L}:\boldsymbol{d}$ are adopted in Secs. 3 and 4, respectively, where $\boldsymbol{T}$ is the second type of P-K stress, $\boldsymbol{L}$ is the elastic tensor, $\boldsymbol{E}$ is the Green strain, $\boldsymbol{\tau}$ is the Kirchhoff stress, $\boldsymbol{d}$ is the deformation rate, and $\overset{\nabla}{()}$ denotes the Janmann rate. The new developed theory with the two types of constitutive models is applied to two classic problems including buckling of an elastic semi-plane solid and buckling of an elastic rectangular solid, respectively. Discussion and Concluding remarks are given in Sec. 5.

2 Finite Prebuckling Deformation Buckling Theory for Bulk Structures

2.1 Kinematics for Finite Deformation of Bulk Structures. Let $\boldsymbol{X}=\boldsymbol{X}(X^A)$ $(A=1, 2, 3)$ be the position of a "material point" in the reference state, where X^A is the Lagrange coordinate. With the vector displacement $\boldsymbol{U}$, the material point $\boldsymbol{X}$ in the reference state moves to $\boldsymbol{x}=\boldsymbol{X}+\boldsymbol{U}$ in the current configuration (Fig. 1). The infinitesimal vector $d\boldsymbol{x}$ becomes

$$d\boldsymbol{x} = d\boldsymbol{X} + d\boldsymbol{U} \tag{1}$$

after the deformation, where $d\boldsymbol{X}$ and $d\boldsymbol{U}$ can be represented as $d\boldsymbol{X}=\boldsymbol{G}_A dX^A$, $d\boldsymbol{U}=\boldsymbol{G}_A dU^A$, respectively. Here, $\boldsymbol{G}_A$ $(A=1, 2, 3)$ are base vectors in the reference state. Substitution of $d\boldsymbol{X}$, $d\boldsymbol{U}$ into Eq. (1) gives

$$d\boldsymbol{x} = dX^A\left(\delta_A^K + \frac{\partial U^K}{\partial X^A}\right)\boldsymbol{G}_K \tag{2}$$

where δ_A^K is the kronecker delta. The definition of the deformation gradient, i.e., $\boldsymbol{F}=\partial\boldsymbol{x}/\partial\boldsymbol{X}$, yields

$$\boldsymbol{F} = \left(\delta_A^K + \frac{\partial U^K}{\partial X^A}\right)\boldsymbol{G}_K\boldsymbol{G}^A \tag{3}$$

The deformation gradient $\boldsymbol{F}$ relates $d\boldsymbol{x}$ and $d\boldsymbol{X}$ by $d\boldsymbol{x} = \boldsymbol{F}\, d\boldsymbol{X}$. The vector of the embedded Lagrange coordinates is then obtained as

$$\hat{\boldsymbol{g}}_A = \frac{\partial \boldsymbol{x}}{\partial X^A} = \left(\delta_A^K + \frac{\partial U^K}{\partial X^A}\right)\boldsymbol{G}_K, \quad A = 1, 2, 3 \tag{4}$$

Comparison of Eqs. (3) and (4) gives $\boldsymbol{F} = \hat{\boldsymbol{g}}_A\boldsymbol{G}^A$. The Green strain tensor is obtained

$$\boldsymbol{E} = \frac{1}{2}(\boldsymbol{F}^T \cdot \boldsymbol{F} - \boldsymbol{1}) \tag{5}$$

by the deformation gradient, where $\boldsymbol{1}$ is the unit tensor.

The present paper focuses on examples of two-dimensional problems with the reference state described by Cartesian coordinates. The basic vectors, coordinates and displacements can be simplified to $\boldsymbol{G}_A = \boldsymbol{G}^A = \boldsymbol{E}_A$, $X^A = X_A$, $U^A = U_A$, $(A = 1, 2)$. The vector of the embedded Lagrange coordinates and the Green strain tensor become

$$\hat{\boldsymbol{g}}_A = \left(\delta_{AK} + \frac{\partial U_K}{\partial X_A}\right)\boldsymbol{E}_K, \quad A = 1, 2 \tag{6}$$

and

$$\boldsymbol{E} = E_{IJ}\boldsymbol{E}_I\boldsymbol{E}_J \tag{7}$$

where

$$\begin{aligned} E_{11} &= \frac{\partial U_1}{\partial X_1} + \frac{1}{2}\left[\left(\frac{\partial U_1}{\partial X_1}\right)^2 + \left(\frac{\partial U_2}{\partial X_1}\right)^2\right] \\ E_{12} = E_{21} &= \frac{1}{2}\left(\frac{\partial U_1}{\partial X_2} + \frac{\partial U_2}{\partial X_1} + \frac{\partial U_1}{\partial X_1}\frac{\partial U_1}{\partial X_2} + \frac{\partial U_2}{\partial X_1}\frac{\partial U_2}{\partial X_2}\right) \\ E_{22} &= \frac{\partial U_2}{\partial X_2} + \frac{1}{2}\left[\left(\frac{\partial U_1}{\partial X_2}\right)^2 + \left(\frac{\partial U_2}{\partial X_2}\right)^2\right] \end{aligned} \tag{8}$$

In Secs. 2.1–2.4 for the finite deformation analysis, all the components must be accurate to the second power of the displacements and their derivatives, as it is the foundation of the buckling analysis. Here, Eq. (8) for Green strain is the accurate expression, and is just right accurate to the second power.

2.2 Constitutive Relations for Finite Deformation of Bulk Structures. Many constitutive models approach the same behavior for small deformation problems. However, buckling are actually problems with the finite deformation. Therefore, the constitutive model must be clear in the framework of finite deformation. In this paper, we will discuss two typical constitutive models and apply them to examples of buckling analysis with significantly different results. One simple constitutive model is the Saint-Venant-Kirchhoff model that the second Piola-Kirchhoff stress $\boldsymbol{T}$ is linearly proportional to the Green strain $\boldsymbol{E}$, i.e.

$$\boldsymbol{T} = \boldsymbol{L}:\boldsymbol{E} \tag{9}$$

Here, $\boldsymbol{L} = (E/1+\nu)\boldsymbol{I} + [\nu E/(1+\nu)(1-2\nu)]\boldsymbol{11}$, where $\boldsymbol{I}$ is the identity tensor, $I_{ijkl} = (\delta_{ik}\delta_{jl} + \delta_{jk}\delta_{il})/2$; $\boldsymbol{1}$ is the unit tensor; E is Young's modulus, and ν is the Poisson's ratio. For two-dimensional problems with Cartesian coordinates, the constitutive relation (9) becomes

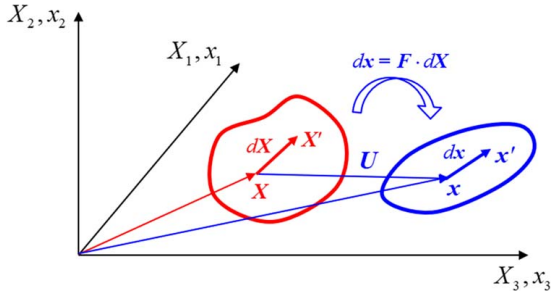

Fig. 1 Schematic illustration for the kinematics of the material point

$$\begin{aligned} T_{11} &= \frac{\overline{E}}{1-\bar{\nu}^2}(E_{11} + \bar{\nu}E_{22}) \\ T_{22} &= \frac{\overline{E}}{1-\bar{\nu}^2}(E_{22} + \bar{\nu}E_{11}) \\ T_{12} = T_{21} &= \frac{\overline{E}}{1+\bar{\nu}}E_{12} = \frac{\overline{E}}{1+\bar{\nu}}E_{21} \end{aligned} \tag{10}$$

Here, $\overline{E} = E$, $\bar{\nu} = \nu$ for plane-stress cases, while $\overline{E} = E/(1-\nu^2)$, $\bar{\nu} = \nu/(1-\nu)$ for plane-strain cases. Another common constitutive model is that the Janmann rate of the Kirchhoff stress $\boldsymbol{\tau}$ is linearly proportional to the deformation rate $\boldsymbol{d}$, i.e., $\overset{\nabla}{\boldsymbol{\tau}} = \boldsymbol{L}:\boldsymbol{d}$, which will be discussed in Sec. 4 separately.

2.3 Equilibrium Equations for Finite Deformation of Bulk Structures. For two-dimensional problems with Cartesian coordinates describing the reference state, the equilibrium equation is

$$\frac{\partial T_{IK}}{\partial X_K} + \hat{\gamma}^I_{KA}T_{AK} = 0, \quad I = 1, 2 \tag{11}$$

where $\hat{\gamma}^I_{KA}$ is second Christoffel symbol of the embedded Lagrange coordinates in the current configuration. $\hat{\gamma}^I_{KA}$ represents the influence of the finite deformation on the equilibrium, and can be obtained by

$$\hat{\gamma}^I_{KA} = \frac{1}{2}g^{LI}\left(\frac{\partial g_{KL}}{\partial X_A} + \frac{\partial g_{AL}}{\partial X_K} - \frac{\partial g_{KA}}{\partial X_L}\right), \quad I, K, A = 1, 2 \tag{12}$$

Here

$$\hat{g}_{AK} = \hat{\boldsymbol{g}}_A \cdot \hat{\boldsymbol{g}}_K = \left(\delta_{AL} + \frac{\partial U_L}{\partial X_A}\right)\left(\delta_{KL} + \frac{\partial U_L}{\partial X_K}\right), \quad A, K = 1, 2 \tag{13}$$

and $\hat{g}^{AK}$ can be obtained by

$$[\hat{g}^{AK}] = [\hat{g}_{AK}]^{-1}, \quad K, A = 1, 2 \tag{14}$$

Using Eqs. (13) and (14), the second Christoffel symbols can be accurately obtained in terms of displacements as

$$
\begin{aligned}
\hat{\gamma}^1_{11} &= \frac{\dfrac{\partial^2 U_1}{\partial X_1^2}+\dfrac{\partial U_2}{\partial X_2}\dfrac{\partial^2 U_1}{\partial X_1^2}-\dfrac{\partial U_1}{\partial X_2}\dfrac{\partial^2 U_2}{\partial X_1^2}}{1+\dfrac{\partial U_1}{\partial X_1}+\dfrac{\partial U_2}{\partial X_2}+\dfrac{\partial U_1}{\partial X_1}\dfrac{\partial U_2}{\partial X_2}-\dfrac{\partial U_1}{\partial X_2}\dfrac{\partial U_2}{\partial X_1}} \\
\hat{\gamma}^1_{12} = \hat{\gamma}^1_{21} &= \frac{\dfrac{\partial^2 U_1}{\partial X_1 \partial X_2}+\dfrac{\partial U_2}{\partial X_2}\dfrac{\partial^2 U_1}{\partial X_1 \partial X_2}-\dfrac{\partial U_1}{\partial X_2}\dfrac{\partial^2 U_2}{\partial X_1 \partial X_2}}{1+\dfrac{\partial U_1}{\partial X_1}+\dfrac{\partial U_2}{\partial X_2}+\dfrac{\partial U_1}{\partial X_1}\dfrac{\partial U_2}{\partial X_2}-\dfrac{\partial U_1}{\partial X_2}\dfrac{\partial U_2}{\partial X_1}} \\
\hat{\gamma}^1_{22} &= \frac{\dfrac{\partial^2 U_1}{\partial X_2^2}+\dfrac{\partial U_2}{\partial X_2}\dfrac{\partial^2 U_1}{\partial X_2^2}-\dfrac{\partial U_1}{\partial X_2}\dfrac{\partial^2 U_2}{\partial X_2^2}}{1+\dfrac{\partial U_1}{\partial X_1}+\dfrac{\partial U_2}{\partial X_2}+\dfrac{\partial U_1}{\partial X_1}\dfrac{\partial U_2}{\partial X_2}-\dfrac{\partial U_1}{\partial X_2}\dfrac{\partial U_2}{\partial X_1}} \\
\hat{\gamma}^2_{11} &= \frac{\dfrac{\partial^2 U_2}{\partial X_1^2}+\dfrac{\partial U_1}{\partial X_1}\dfrac{\partial^2 U_2}{\partial X_1^2}-\dfrac{\partial U_2}{\partial X_1}\dfrac{\partial^2 U_1}{\partial X_1^2}}{1+\dfrac{\partial U_1}{\partial X_1}+\dfrac{\partial U_2}{\partial X_2}+\dfrac{\partial U_1}{\partial X_1}\dfrac{\partial U_2}{\partial X_2}-\dfrac{\partial U_1}{\partial X_2}\dfrac{\partial U_2}{\partial X_1}} \\
\hat{\gamma}^2_{12} = \hat{\gamma}^2_{21} &= \frac{\dfrac{\partial^2 U_2}{\partial X_1 \partial X_2}+\dfrac{\partial U_1}{\partial X_1}\dfrac{\partial^2 U_2}{\partial X_1 \partial X_2}-\dfrac{\partial U_2}{\partial X_1}\dfrac{\partial^2 U_1}{\partial X_1 \partial X_2}}{1+\dfrac{\partial U_1}{\partial X_1}+\dfrac{\partial U_2}{\partial X_2}+\dfrac{\partial U_1}{\partial X_1}\dfrac{\partial U_2}{\partial X_2}-\dfrac{\partial U_1}{\partial X_2}\dfrac{\partial U_2}{\partial X_1}} \\
\hat{\gamma}^2_{22} &= \frac{\dfrac{\partial^2 U_2}{\partial X_2^2}+\dfrac{\partial U_1}{\partial X_1}\dfrac{\partial^2 U_2}{\partial X_2^2}-\dfrac{\partial U_2}{\partial X_1}\dfrac{\partial^2 U_1}{\partial X_2^2}}{1+\dfrac{\partial U_1}{\partial X_1}+\dfrac{\partial U_2}{\partial X_2}+\dfrac{\partial U_1}{\partial X_1}\dfrac{\partial U_2}{\partial X_2}-\dfrac{\partial U_1}{\partial X_2}\dfrac{\partial U_2}{\partial X_1}}
\end{aligned} \tag{15}
$$

Assume that the displacements U_1 and U_2 are at the same order, Eq. (15) can be expanded as

$$
\begin{aligned}
\hat{\gamma}^1_{11} &= \frac{\partial^2 U_1}{\partial X_1^2}-\left[\frac{\partial U_1}{\partial X_1}\frac{\partial^2 U_1}{\partial X_1^2}+\frac{\partial U_1}{\partial X_2}\frac{\partial^2 U_2}{\partial X_1^2}\right]+\cdots \\
\hat{\gamma}^1_{12} = \hat{\gamma}^1_{21} &= \frac{\partial^2 U_1}{\partial X_1 \partial X_2}-\left[\frac{\partial U_1}{\partial X_1}\frac{\partial^2 U_1}{\partial X_1 \partial X_2}+\frac{\partial U_1}{\partial X_2}\frac{\partial^2 U_2}{\partial X_1 \partial X_2}\right]+\cdots \\
\hat{\gamma}^1_{22} &= \frac{\partial^2 U_1}{\partial X_2^2}-\left[\frac{\partial U_1}{\partial X_2}\frac{\partial^2 U_2}{\partial X_2^2}+\frac{\partial U_1}{\partial X_1}\frac{\partial^2 U_1}{\partial X_2^2}\right]+\cdots \\
\hat{\gamma}^2_{11} &= \frac{\partial^2 U_2}{\partial X_1^2}-\left[\frac{\partial^2 U_2}{\partial X_1^2}\frac{\partial U_2}{\partial X_2}+\frac{\partial^2 U_1}{\partial X_1^2}\frac{\partial U_2}{\partial X_1}\right]+\cdots \\
\hat{\gamma}^2_{12} = \hat{\gamma}^2_{21} &= \frac{\partial^2 U_2}{\partial X_1 \partial X_2}-\left[\frac{\partial^2 U_2}{\partial X_1 \partial X_2}\frac{\partial U_2}{\partial X_2}+\frac{\partial^2 U_1}{\partial X_1 \partial X_2}\frac{\partial U_2}{\partial X_1}\right]+\cdots \\
\hat{\gamma}^2_{22} &= \frac{\partial^2 U_2}{\partial X_2^2}-\left[\frac{\partial^2 U_2}{\partial X_2^2}\frac{\partial U_2}{\partial X_2}+\frac{\partial^2 U_1}{\partial X_2^2}\frac{\partial U_2}{\partial X_1}\right]+\cdots
\end{aligned} \tag{16}
$$

Substitution of Eq. (16) into Eq. (11), together with constitutive Eq. (10), yields the equilibrium equations in terms of displacements for finite deformation problems, as well as buckling problems.

2.4 Boundary Conditions for Finite Deformation of Bulk Structures. It is worth to study the stress/force boundary conditions for finite deformation problems. Most of boundary conditions should be established in the current configuration, since the structures equilibrate in this state. The traction-free boundary condition is

$$
\boldsymbol{\sigma} \cdot d\boldsymbol{a} = 0 \tag{17}
$$

Here $\boldsymbol{\sigma}$ is the Cauchy stress, which is the so-called real stress; $d\boldsymbol{a}$ is infinitesimal area of the traction-free surface in the current configuration. Equation (17) can be transfer to the formulate in terms of second type of P-K stress as

$$
\boldsymbol{\sigma} \cdot d\boldsymbol{a} = \boldsymbol{F} \cdot \boldsymbol{T} \cdot d\boldsymbol{A} = 0 \tag{18}
$$

which is convenient to use, considering the expression of the constitutive relations and equilibrium equation in the above paragraphs.

2.5 Buckling Analysis Considering the Effect of Finite Prebuckling Deformation. As we discussed in preceding paper [13], the buckling process undergoes four regimes including the original regime without any load, the onset of buckling subject to the critical buckling load, the buckling regime subject to the critical buckling load and postbuckling under increasing/decreasing load. The regime at the onset of buckling should be studied before the buckling analysis. Let $\overset{\circ}{\boldsymbol{U}}$, $\overset{\circ}{\boldsymbol{E}}$, $\overset{\circ}{\boldsymbol{T}}$, and $\hat{\gamma}^{\circ I}_{KA}$ denote the displacements, the Green strain, the second Piola-Kirchhoff stress, and the second Christoffel symbols at the onset of buckling. Here and in the following, "$\circ$" denotes the variables at the onset of buckling. According to Eqs. (8), (10), (11), and (16), it is straightforward to obtain the governing equations at the onset of buckling, including the geometric equations

$$
\begin{aligned}
\overset{\circ}{E}_{11} &= \frac{\partial \overset{\circ}{U}_1}{\partial X_1}+\cdots \\
\overset{\circ}{E}_{12} = \overset{\circ}{E}_{21} &= \frac{1}{2}\left(\frac{\partial \overset{\circ}{U}_1}{\partial X_2}+\frac{\partial \overset{\circ}{U}_2}{\partial X_1}+\cdots\right) \\
\overset{\circ}{E}_{22} &= \frac{\partial \overset{\circ}{U}_2}{\partial X_2}+\cdots
\end{aligned} \tag{19}
$$

the constitutive equations

$$
\begin{aligned}
\overset{\circ}{T}_{11} &= \frac{\overline{E}}{1-\bar{\nu}^2}\left(\overset{\circ}{E}_{11}+\bar{\nu}\overset{\circ}{E}_{22}\right) \\
\overset{\circ}{T}_{22} &= \frac{\overline{E}}{1-\bar{\nu}^2}\left(\overset{\circ}{E}_{22}+\bar{\nu}\overset{\circ}{E}_{11}\right) \\
\overset{\circ}{T}_{12} = \overset{\circ}{T}_{21} &= \frac{\overline{E}}{1+\bar{\nu}}\overset{\circ}{E}_{12} = \frac{\overline{E}}{1+\bar{\nu}}\overset{\circ}{E}_{21}
\end{aligned} \tag{20}
$$

and the equilibrium equations

$$
\frac{\partial \overset{\circ}{T}_{IK}}{\partial X_K}+\cdots = 0, \quad I = 1, 2 \tag{21}
$$

Here, Eqs. (19)–(21) are accurate to the first power of displacements for all the components. They are actually the governing equations for linear elastic problems.

Substitution of $\boldsymbol{U} = \overset{\circ}{\boldsymbol{U}}+\Delta\boldsymbol{U}$, $\boldsymbol{E} = \overset{\circ}{\boldsymbol{E}}+\Delta\boldsymbol{E}$, $\boldsymbol{T} = \overset{\circ}{\boldsymbol{T}}+\Delta\boldsymbol{T}$, and $\hat{\gamma}^I_{KA} = \hat{\gamma}^{\circ I}_{KA}+\Delta\hat{\gamma}^I_{KA}$ into Eqs. (8), (10), (11), and (16) yield the equations for the regime after buckling, which together with Eqs. (19)–(21), result the governing equations for the critical buckling behaviors. The yielded geometric equations, constitutive equations and equilibrium equations are

$$
\begin{aligned}
\Delta E_{11} &= \left(1+\underline{\frac{\partial \overset{\circ}{U}_1}{\partial X_1}}\right)\frac{\partial \Delta U_1}{\partial X_1}+\underline{\frac{\partial \overset{\circ}{U}_2}{\partial X_1}}\frac{\partial \Delta U_2}{\partial X_1}+\cdots \\
\Delta E_{12} = \Delta E_{21} &= \frac{1}{2}\left[\left(1+\underline{\frac{\partial \overset{\circ}{U}_1}{\partial X_1}}\right)\frac{\partial \Delta U_1}{\partial X_2}+\left(1+\underline{\frac{\partial \overset{\circ}{U}_2}{\partial X_2}}\right)\frac{\partial \Delta U_2}{\partial X_1}\right. \\
&\quad \left.+\underline{\frac{\partial \overset{\circ}{U}_1}{\partial X_2}}\frac{\partial \Delta U_1}{\partial X_1}+\underline{\frac{\partial \overset{\circ}{U}_2}{\partial X_1}}\frac{\partial \Delta U_2}{\partial X_2}+\cdots\right] \\
\Delta E_{22} &= \left(1+\underline{\frac{\partial \overset{\circ}{U}_2}{\partial X_2}}\right)\frac{\partial \Delta U_2}{\partial X_2}+\underline{\frac{\partial \overset{\circ}{U}_1}{\partial X_2}}\frac{\partial \Delta U_1}{\partial X_2}+\cdots
\end{aligned} \tag{22}
$$

$$\Delta T_{11}=\frac{\overline{E}}{1-\bar{\nu}^2}(\Delta E_{11}+\bar{\nu}\Delta E_{22})$$
$$\Delta T_{22}=\frac{\overline{E}}{1-\bar{\nu}^2}(\Delta E_{22}+\bar{\nu}\Delta E_{11}) \tag{23}$$
$$\Delta T_{12}=\Delta T_{21}=\frac{\overline{E}}{1+\bar{\nu}}\Delta E_{12}=\frac{\overline{E}}{1+\bar{\nu}}\Delta E_{21}$$

and

$$\frac{\partial \Delta T_{IK}}{\partial X_K}+\Delta\hat{\gamma}^I_{KA}\overset{\circ}{T}_{AK}+\underline{\hat{\gamma}^{\circ I}_{KA}}\Delta T_{AK}+\cdots=0,\quad I=1,2 \tag{24}$$

respectively, where

$$\hat{\gamma}^{\circ 1}_{11}=\frac{\partial^2\overset{\circ}{U}_1}{\partial X_1^2}+\cdots\quad \hat{\gamma}^{\circ 1}_{12}=\hat{\gamma}^{\circ 1}_{21}=\frac{\partial^2\overset{\circ}{U}_1}{\partial X_1\partial X_2}+\cdots$$
$$\hat{\gamma}^{\circ 1}_{22}=\frac{\partial^2\overset{\circ}{U}_1}{\partial X_2^2}+\cdots\quad \hat{\gamma}^{\circ 2}_{11}=\frac{\partial^2\overset{\circ}{U}_2}{\partial X_1^2}+\cdots \tag{25}$$
$$\hat{\gamma}^{\circ 2}_{12}=\hat{\gamma}^{\circ 2}_{21}=\frac{\partial^2\overset{\circ}{U}_2}{\partial X_1\partial X_2}+\cdots\quad \hat{\gamma}^{\circ 2}_{22}=\frac{\partial^2\overset{\circ}{U}_2}{\partial X_2^2}+\cdots$$

and

$$\Delta\hat{\gamma}^1_{11}=\left(1-\frac{\partial\overset{\circ}{U}_1}{\underline{\partial X_1}}\right)\frac{\partial^2\Delta U_1}{\partial X_1^2}-\frac{\partial^2\overset{\circ}{U}_1}{\underline{\partial X_1^2}}\frac{\partial\Delta U_1}{\partial X_1}-\frac{\partial\overset{\circ}{U}_1}{\underline{\partial X_2}}\frac{\partial^2\Delta U_2}{\partial X_1^2}-\frac{\partial^2\overset{\circ}{U}_2}{\underline{\partial X_1^2}}\frac{\partial\Delta U_1}{\partial X_2}+\cdots$$
$$\Delta\hat{\gamma}^1_{12}=\hat{\gamma}^1_{21}=\left(1-\frac{\partial\overset{\circ}{U}_1}{\underline{\partial X_1}}\right)\frac{\partial^2\Delta U_1}{\partial X_1\partial X_2}-\frac{\partial^2\overset{\circ}{U}_1}{\underline{\partial X_1\partial X_2}}\frac{\partial\Delta U_1}{\partial X_1}-\frac{\partial\overset{\circ}{U}_1}{\underline{\partial X_2}}\frac{\partial^2\Delta U_2}{\partial X_1\partial X_2}-\frac{\partial^2\overset{\circ}{U}_2}{\underline{\partial X_1\partial X_2}}\frac{\partial\Delta U_1}{\partial X_2}+\cdots$$
$$\Delta\hat{\gamma}^1_{22}=\left(1-\frac{\partial\overset{\circ}{U}_1}{\underline{\partial X_1}}\right)\frac{\partial^2\Delta U_1}{\partial X_2^2}-\frac{\partial\overset{\circ}{U}_1}{\underline{\partial X_2}}\frac{\partial^2\Delta U_2}{\partial X_2^2}-\frac{\partial^2\overset{\circ}{U}_2}{\underline{\partial X_2^2}}\frac{\partial\Delta U_1}{\partial X_2}-\frac{\partial^2\overset{\circ}{U}_1}{\underline{\partial X_2^2}}\frac{\partial\Delta U_1}{\partial X_1}+\cdots$$
$$\Delta\hat{\gamma}^2_{11}=\left(1-\frac{\partial\overset{\circ}{U}_2}{\underline{\partial X_2}}\right)\frac{\partial^2\Delta U_2}{\partial X_1^2}-\frac{\partial^2\overset{\circ}{U}_2}{\underline{\partial X_1^2}}\frac{\partial\Delta U_2}{\partial X_2}-\frac{\partial\overset{\circ}{U}_2}{\underline{\partial X_1}}\frac{\partial^2\Delta U_1}{\partial X_1^2}-\frac{\partial^2\overset{\circ}{U}_1}{\underline{\partial X_1^2}}\frac{\partial\Delta U_2}{\partial X_1}+\cdots \tag{26}$$
$$\Delta\hat{\gamma}^2_{12}=\hat{\gamma}^2_{21}=\left(1-\frac{\partial\overset{\circ}{U}_2}{\underline{\partial X_2}}\right)\frac{\partial^2\Delta U_2}{\partial X_1\partial X_2}-\frac{\partial^2\overset{\circ}{U}_2}{\underline{\partial X_1\partial X_2}}\frac{\partial\Delta U_2}{\partial X_2}-\frac{\partial\overset{\circ}{U}_2}{\underline{\partial X_1}}\frac{\partial^2\Delta U_1}{\partial X_1\partial X_2}-\frac{\partial^2\overset{\circ}{U}_1}{\underline{\partial X_1\partial X_2}}\frac{\partial\Delta U_2}{\partial X_1}+\cdots$$
$$\Delta\hat{\gamma}^2_{22}=\left(1-\frac{\partial\overset{\circ}{U}_2}{\underline{\partial X_2}}\right)\frac{\partial^2\Delta U_2}{\partial X_2^2}-\frac{\partial^2\overset{\circ}{U}_2}{\underline{\partial X_2^2}}\frac{\partial\Delta U_2}{\partial X_2}-\frac{\partial^2\overset{\circ}{U}_1}{\underline{\partial X_2^2}}\frac{\partial\Delta U_2}{\partial X_1}-\frac{\partial\overset{\circ}{U}_2}{\underline{\partial X_1}}\frac{\partial^2\Delta U_1}{\partial X_2^2}+\cdots$$

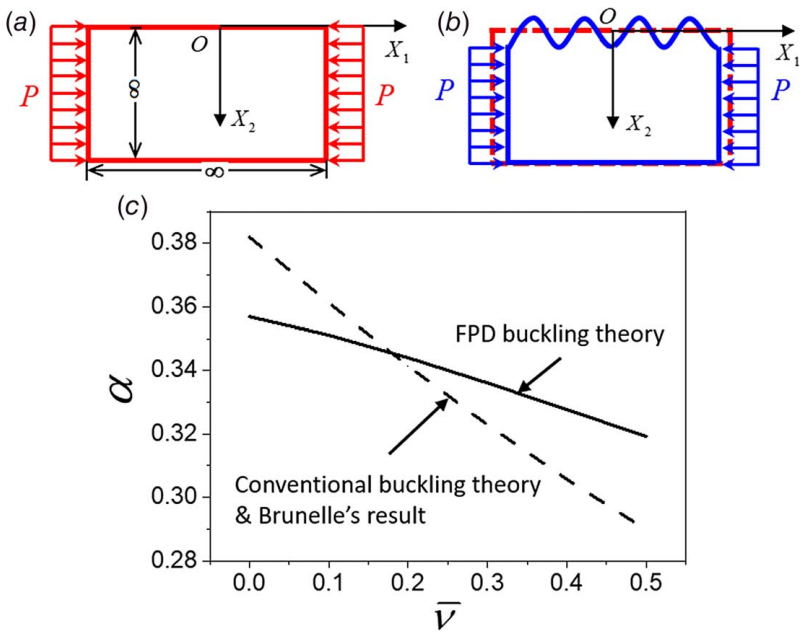

Fig. 2 Buckling analysis of the elastic semi-plane solid with the constitutive model T = L:E. The (*a*) undeformed, (*b*) buckling modes, and (*c*) The curves of the dimensionless critical buckling load α versus the Poisson's ratio $\bar{\nu}$ for the FPD buckling theory, the CBT and E. J. Brunelle's result

It is worth to point out that the critical buckling analysis needs to account for all terms up to only the first power of displacement (with "Δ") in the deformation components. On the other hand, the variables with "o" serve as the coefficients of the incremental terms. These coefficients are also accurate to the first power of the variables with "o". The underlined terms in the above and following equations are for the effect of the prebuckling deformation, which are neglected by the CBT and conventional numerical method (CNM). Here, they are considered for FPD buckling problems.

3 Examples With the Saint-Venant-Kirchhoff Model

3.1 Buckling of an Elastic Semi-Plane Solid Subject to Compression. Buckling of an elastic semi-plane solid subject to compression is a classic problem that has been studied by Brunelle [20] and Biot and Drucker [44]. Figures 2(*a*) and 2(*b*) illustrate the modes before and after buckling, respectively. It is easy to obtain the stress distribution at the onset of buckling

$$\overset{\circ}{T}_{11} = -P, \quad \overset{\circ}{T}_{12} = \overset{\circ}{T}_{21} = 0, \quad \overset{\circ}{T}_{22} = 0 \tag{27}$$

Substitution of Eq. (26) into Eq. (20), together with Eq. (19), gives

$$\frac{\partial \overset{\circ}{U}_1}{\partial X_1} = -\frac{P}{\overline{E}}, \quad \frac{\partial \overset{\circ}{U}_1}{\partial X_2} = 0, \quad \frac{\partial \overset{\circ}{U}_2}{\partial X_1} = 0, \quad \frac{\partial \overset{\circ}{U}_2}{\partial X_2} = \frac{\bar{\nu}P}{\overline{E}} \tag{28}$$

Here, it is not necessary to compute the displacements, since the following buckling analysis requires their derivatives only.

Using Eqs. (27) and (28), Eqs. (24)–(26) give the expanded equilibrium equations as

$$\begin{aligned} &\frac{\partial \Delta T_{11}}{\partial X_1} + \frac{\partial \Delta T_{12}}{\partial X_2} - P\left(1 - \frac{\partial \overset{\circ}{U}_1}{\underline{\partial X_1}}\right)\frac{\partial^2 \Delta U_1}{\partial X_1^2} = 0 \\ &\frac{\partial \Delta T_{22}}{\partial X_2} + \frac{\partial \Delta T_{21}}{\partial X_1} - P\left(1 - \frac{\partial \overset{\circ}{U}_2}{\underline{\partial X_2}}\right)\frac{\partial^2 \Delta U_2}{\partial X_1^2} = 0 \end{aligned} \tag{29}$$

The combination of Eqs. (22), (23), and (29) yields the equilibrium equations in terms of the displacements

$$\begin{aligned} &\frac{\overline{E}}{1-\bar{\nu}^2}\frac{\partial}{\partial X_1}\left[\left(1 + \frac{\partial \overset{\circ}{U}_1}{\underline{\partial X_1}}\right)\frac{\partial \Delta U_1}{\partial X_1} + \bar{\nu}\left(1 + \frac{\partial \overset{\circ}{U}_2}{\underline{\partial X_2}}\right)\frac{\partial \Delta U_2}{\partial X_2}\right] \\ &+ \frac{\overline{E}}{1+\bar{\nu}}\frac{\partial}{\partial X_2}\frac{1}{2}\left[\left(1 + \frac{\partial \overset{\circ}{U}_1}{\underline{\partial X_1}}\right)\frac{\partial \Delta U_1}{\partial X_2} + \left(1 + \frac{\partial \overset{\circ}{U}_2}{\underline{\partial X_2}}\right)\frac{\partial \Delta U_2}{\partial X_1}\right] \\ &- P\left(1 - \frac{\partial \overset{\circ}{U}_1}{\underline{\partial X_1}}\right)\frac{\partial^2 \Delta U_1}{\partial X_1^2} = 0 \\ &\frac{\overline{E}}{1+\bar{\nu}}\frac{\partial}{\partial X_1}\frac{1}{2}\left[\left(1 + \frac{\partial \overset{\circ}{U}_1}{\underline{\partial X_1}}\right)\frac{\partial \Delta U_1}{\partial X_2} + \left(1 + \frac{\partial \overset{\circ}{U}_2}{\underline{\partial X_2}}\right)\frac{\partial \Delta U_2}{\partial X_1}\right] \\ &+ \frac{\overline{E}}{1-\bar{\nu}^2}\frac{\partial}{\partial X_2}\left[\left(1 + \frac{\partial \overset{\circ}{U}_2}{\underline{\partial X_2}}\right)\frac{\partial \Delta U_2}{\partial X_2} + \bar{\nu}\left(1 + \frac{\partial \overset{\circ}{U}_1}{\underline{\partial X_1}}\right)\frac{\partial \Delta U_1}{\partial X_1}\right] \\ &- P\left(1 - \frac{\partial \overset{\circ}{U}_2}{\underline{\partial X_2}}\right)\frac{\partial^2 \Delta U_2}{\partial X_1^2} = 0 \end{aligned} \tag{30}$$

Let

$$\alpha = \frac{P}{\overline{E}} \tag{31}$$

be the dimensionless critical buckling load. Using Eq. (28), the derivatives of displacements can also be expressed in terms of α

$$\frac{\partial \overset{\circ}{U}_1}{\partial X_1} = -\alpha, \quad \frac{\partial \overset{\circ}{U}_2}{\partial X_2} = \bar{\nu}\alpha \tag{32}$$

Here, the same standard holds. Variables with "o", as the coefficients in the differential equations, are accurate to the first power. Substitution of Eqs. (31) and (32) into Eq. (30) yields

$$\begin{aligned} &[(1-\underline{\alpha}) - \alpha(1-\bar{\nu}^2)]\frac{\partial^2 \Delta U_1}{\partial X_1^2} + \frac{1-\bar{\nu}}{2}(1-\underline{\alpha})\frac{\partial^2 \Delta U_1}{\partial X_2^2} + \frac{1+\bar{\nu}}{2}(1+\underline{\bar{\nu}\alpha})\frac{\partial^2 \Delta U_2}{\partial X_1 \partial X_2} = 0 \\ &\left[\frac{1-\bar{\nu}}{2}(1+\underline{\bar{\nu}\alpha}) - \alpha(1-\bar{\nu}^2)\right]\frac{\partial^2 \Delta U_2}{\partial X_1^2} + (1+\underline{\bar{\nu}\alpha})\frac{\partial^2 \Delta U_2}{\partial X_2^2} + \frac{1+\bar{\nu}}{2}(1-\underline{\alpha})\frac{\partial^2 \Delta U_1}{\partial X_1 \partial X_2} = 0 \end{aligned} \tag{33}$$

The general solution of Eq. (33) is

$$\begin{aligned} \Delta U_1 &= \sin(kX_1)[C_1\cosh(b_1 kX_2) + C_2\sinh(b_1 kX_2) + C_3\cosh(b_2 kX_2) + C_4\sinh(b_2 kX_2)] \\ \Delta U_2 &= \cos(kX_1)[D_1\sinh(b_1 kX_2) + D_2\cosh(b_1 kX_2) + D_3\sinh(b_2 kX_2) + D_4\cosh(b_2 kX_2)] \end{aligned} \tag{34}$$

where k, b_1, b_2, $C_1 \sim C_4$, and $D_1 \sim D_4$ are the coefficients to be determined. Here, only even functions about X_1 are used for ΔU_2, without the universality of the problem. Substitution of solution (34) into Eq. (33) gives

$$\begin{aligned} b_1 &= \sqrt{\frac{\left\{(\bar{\nu}^2 - 2\bar{\nu} - 3)\alpha + 2\underline{+(-3\bar{\nu}^2 - 4\bar{\nu} + 1)\alpha^2 + (2\bar{\nu} - 2)\alpha} \right. \\ &\qquad \left. \underline{+\sqrt{(\bar{\nu}+1)^3[(\bar{\nu}+1)\alpha^2 + (5\bar{\nu}+1)\alpha^4 + (6-2\bar{\nu})\alpha^3 - 4\alpha^2]}}\right\}}{2(1\underline{-\bar{\nu}\alpha^2 + \bar{\nu}\alpha - \alpha})} \\ b_2 &= \sqrt{\frac{\left\{(\bar{\nu}^2 - 2\bar{\nu} - 3)\alpha + 2\underline{+(-3\bar{\nu}^2 - 4\bar{\nu} + 1)\alpha^2 + (2\bar{\nu} - 2)\alpha} \right. \\ &\qquad \left. \underline{-\sqrt{(\bar{\nu}+1)^3[(\bar{\nu}+1)\alpha^2 + (5\bar{\nu}+1)\alpha^4 + (6-2\bar{\nu})\alpha^3 - 4\alpha^2]}}\right\}}{2(1\underline{-\bar{\nu}\alpha^2 + \bar{\nu}\alpha - \alpha})} \end{aligned} \tag{35}$$

The relations between the coefficients in solution (34) needs to satisfy

$$D_1 = N_1 C_1,\ D_2 = N_1 C_2,\ D_3 = N_2 C_3,\ D_4 = N_2 C_4 \tag{36}$$

where

$$N_1 = \frac{b_1(\bar{\nu}+1)(\underline{\alpha}-1)}{(2-2\bar{\nu}^2)\alpha + 2b_1^2 + \bar{\nu} - 1 \underline{+(2\bar{\nu}b_1^2 + \bar{\nu}^2 - \bar{\nu})\alpha}}$$
$$N_2 = \frac{b_2(\bar{\nu}+1)(\underline{\alpha}-1)}{(2-2\bar{\nu}^2)\alpha + 2b_2^2 + \bar{\nu} - 1 \underline{+(2\bar{\nu}b_2^2 + \bar{\nu}^2 - \bar{\nu})\alpha}} \tag{37}$$

The boundary condition at $X_2 \to \infty$ requires that

$$\lim_{X_2\to\infty} \Delta U_1 = \lim_{X_2\to\infty} \Delta U_2 = 0 \tag{38}$$

which yields

$$C_2 = -C_1,\ C_4 = -C_3,\ D_2 = -D_1,\ D_4 = -D_3 \tag{39}$$

Substitution of solution (36) and (39) into Eq. (34) gives

$$\Delta U_1 = \sin(kX_1)[C_1 e^{-b_1 kX_2} + C_3 e^{-b_2 kX_2}]$$
$$\Delta U_2 = \cos(kX_1)[-N_1 C_1 e^{-b_1 kX_2} - N_2 C_3 e^{-b_2 kX_2}] \tag{40}$$

The traction-free condition at $X_2 = 0$ requires

$$\boldsymbol{\sigma}\cdot d\boldsymbol{a}|_{X_2=0} = \boldsymbol{F}\cdot\boldsymbol{T}\cdot(dA_2\boldsymbol{E}_2)|_{X_2=0} = 0 \tag{41}$$

which yields

$$\left(\underline{\mathring{T}_{12}} + \Delta T_{12}\right) + \left(\underline{\frac{\partial \mathring{U}_1}{\partial X_1}} + \frac{\partial \Delta U_1}{\partial X_1}\right)\left(\underline{\mathring{T}_{12}} + \Delta T_{12}\right)$$
$$+ \left(\underline{\frac{\partial \mathring{U}_1}{\partial X_2}} + \frac{\partial \Delta U_1}{\partial X_2}\right)\left(\underline{\mathring{T}_{22}} + \Delta T_{22}\right) = 0$$
$$\left(\underline{\mathring{T}_{22}} + \Delta T_{22}\right) + \left(\underline{\frac{\partial \mathring{U}_2}{\partial X_2}} + \frac{\partial \Delta U_2}{\partial X_2}\right)\left(\underline{\mathring{T}_{22}} + \Delta T_{22}\right) \tag{42}$$
$$+ \left(\underline{\frac{\partial \mathring{U}_2}{\partial X_1}} + \frac{\partial \Delta U_2}{\partial X_1}\right)\left(\underline{\mathring{T}_{12}} + \Delta T_{12}\right) = 0$$

Using Eqs. (22), (23), (27), and (32), Eq. (42) becomes

$$\begin{matrix}(1-\underline{\alpha})\dfrac{\partial \Delta U_1}{\partial X_2} + (1+\underline{\bar{\nu}\alpha})\dfrac{\partial \Delta U_2}{\partial X_1} = 0 \\ (1+\underline{\bar{\nu}\alpha})\dfrac{\partial \Delta U_2}{\partial X_2} + \bar{\nu}(1-\underline{\alpha})\dfrac{\partial \Delta U_1}{\partial X_1} = 0\end{matrix},\ \text{at } X_2 = 0 \tag{43}$$

The solution (40) needs to satisfy the requirements (43), i.e.

$$\begin{bmatrix}(1+\underline{\bar{\nu}\alpha})N_1 - (1-\underline{\alpha})b_1 & (1+\underline{\bar{\nu}\alpha})N_2 - (1-\underline{\alpha})b_2 \\ (1+\underline{\bar{\nu}\alpha})N_1 b_1 + (1-\underline{\alpha})\bar{\nu} & (1+\underline{\bar{\nu}\alpha})N_2 b_2 + (1-\underline{\alpha})\bar{\nu}\end{bmatrix}\begin{pmatrix}C_1 \\ C_3\end{pmatrix} = 0 \tag{44}$$

The determinant of the coefficient matrix of Eq. (44) must be zero for nontrivial solution. It requires

$$[(1+\underline{\bar{\nu}\alpha})N_1 b_1 + (1-\underline{\alpha})\bar{\nu}][(1+\underline{\bar{\nu}\alpha})N_2 - (1-\underline{\alpha})b_2]$$
$$-[(1+\underline{\bar{\nu}\alpha})N_2 b_2 + (1-\underline{\alpha})\bar{\nu}][(1+\underline{\bar{\nu}\alpha})N_1 - (1-\underline{\alpha})b_1] = 0 \tag{45}$$

the solution of which gives the dimensionless critical buckling load α. In Eq. (45), it is found that there is only one physical solution for α without higher-order solutions. On the other hand, Eq. (45) is independent of the parameter k, which exists in the expressions (34) and (40) for sinusoidal buckling modes. It means that, for the buckling problem of the elastic semi-plane solid, there is only one critical buckling load which corresponds to infinite sinusoidal buckling modes. It is worth mentioning that the postbuckling analysis reveals that sinusoidal buckling mode may be unstable and imperfection-sensitive [45]. On one hand, for structures with no imperfection, the sinusoidal buckling mode may switch to the creasing mode under the external disturbance or the occurrence of plasticity. On the other hand, the creasing mode may also appear when the initial imperfection exists in the structure. In the present paper, we focus on the FPD buckling behaviors for the sinusoidal buckling modes, the critical buckling load of which can be determined by the linear buckling analysis. The study of the buckling mode selection by FPD buckling theory will be discussed in the future work.

Without the consideration of the prebuckling deformation (CBT), the terms with underlines are neglected. The equilibrium Eq. (33) and the boundary conditions (43) become

$$\frac{\partial^2 \Delta U_1}{\partial X_1^2} + \frac{1-\bar{\nu}}{2}\frac{\partial^2 \Delta U_1}{\partial X_2^2} + \frac{1+\bar{\nu}}{2}\frac{\partial^2 \Delta U_2}{\partial X_1 \partial X_2} - \alpha(1-\bar{\nu}^2)\frac{\partial^2 \Delta U_1}{\partial X_1^2} = 0$$
$$\frac{\partial^2 \Delta U_2}{\partial X_2^2} + \frac{1-\bar{\nu}}{2}\frac{\partial^2 \Delta U_2}{\partial X_1^2} + \frac{1+\bar{\nu}}{2}\frac{\partial^2 \Delta U_1}{\partial X_1 \partial X_2} - \alpha(1-\bar{\nu}^2)\frac{\partial^2 \Delta U_2}{\partial X_1^2} = 0 \tag{46}$$

and

$$\begin{matrix}\dfrac{\partial \Delta U_1}{\partial X_2} + \dfrac{\partial \Delta U_2}{\partial X_1} = 0 \\ \dfrac{\partial \Delta U_2}{\partial X_2} + \bar{\nu}\dfrac{\partial \Delta U_1}{\partial X_1} = 0\end{matrix},\ \text{at } X_2 = 0 \tag{47}$$

respectively. The requirement (45) for the critical buckling load is reduced to

$$(N_1 b_1 + \bar{\nu})(N_2 - b_2) - (N_2 b_2 + \bar{\nu})(N_1 - b_1) = 0 \tag{48}$$

and can be further simplified to

$$(\bar{\nu}^2 + 2\bar{\nu} + 1)\alpha^3 - (4\bar{\nu} + 4)\alpha^2 + (2\bar{\nu} + 4)\alpha - 1 = 0 \tag{49}$$

The solution for the lowest dimensionless critical buckling load is obtained analytically as

$$\alpha = \begin{cases} \dfrac{4 - 2\sqrt{4-6\bar{\nu}}\cos\left(\frac{1}{3}\arccos\left(\frac{\sqrt{2}(45\bar{\nu}-11)}{8\sqrt{(-3\bar{\nu}+2)^3}}\right)\right)}{3(\bar{\nu}+1)}, & \text{for } 96\bar{\nu}^3 + 33\bar{\nu}^2 + 18\bar{\nu} - 15 < 0 \\ -\dfrac{\left[\begin{array}{l}\left(12\sqrt{96\bar{\nu}^3 + 33\bar{\nu}^2 + 18\bar{\nu} - 15} + 180\bar{\nu} - 44\right)^{1/3} \\ +\left(-12\sqrt{96\bar{\nu}^3 + 33\bar{\nu}^2 + 18\bar{\nu} - 15} + 180\bar{\nu} - 44\right)^{1/3}\end{array}\right]}{6(\bar{\nu}+1)} + \dfrac{4}{3(\bar{\nu}+1)}, & \text{for } 96\bar{\nu}^3 + 33\bar{\nu}^2 + 18\bar{\nu} - 15 \geq 0 \end{cases} \tag{50}$$

which agrees well with the results by Brunelle [20]. For comparison, Ogden's theory [26] is applied to the buckling of an elastic semi-plane solid with the Saint-Venant-Kirchhoff constitutive model (the details of the derivation are shown in Appendix B). It is found that for $\alpha \ll 1$, the equilibrium equations and the boundary condition of the Ogden's theory are same with Eqs. (33) and (43) in the FPD buckling theory, respectively.

While there is not any dimension parameter for the elastic semi-plane solid, the only variable parameter is the material property, i.e., the Poisson's ratio $\bar{\nu}$. Figure 2(*c*) shows the comparison of the dimensionless critical buckling load α versus the Poisson's ratio. The solid line shows the result from Eq. (45) by FPD buckling theory for bulk structures. The dimensionless critical buckling load α decreases with the increase of the Poisson's ratio $\bar{\nu}$. For comparison, the dashed line gives the result from Eq. (50) by the CBT without the consideration of the effects of finite prebuckling deformation, which is consistent with the results by Brunelle [20]. The maximum error yielded by the neglect of the finite prebuckling deformation is about 10%, which occurs at $\bar{\nu} \to 0.5$.

3.2 Buckling of an Elastic Rectangular Solid Subject to Compression. Buckling of an elastic rectangular solid subject to compression is another classic problem [19]. It degenerates to Euler buckling, which is the most famous buckling problem, if the aspect ratio is large [1]. Here, our theory is also applied in the follows. Consider an elastic rectangular solid subject to pressure P, as depicted in Fig. 3(*a*). Its buckling mode shown in Fig. 3(*b*) is similar to that of slender beams, but without the assumption of the plane section.

The analysis from Eqs. (27) to (37) also works here. The boundary conditions require that

$$\Delta U_1|_{X_1=\pm L/2} = 0 \tag{51}$$

Substitution of solution (34) into Eq. (51) yields

$$k = \frac{2\pi}{L} \tag{52}$$

which, together with Eq. (36) gives

$$\begin{aligned}
\Delta U_1 &= \sin\left(2\pi\frac{X_1}{L}\right)\\
&\left[\begin{array}{l} C_1\cosh\left(2\pi b_1\frac{X_2}{L}\right) + C_2\sinh\left(2\pi b_1\frac{X_2}{L}\right)\\ +C_3\cosh\left(2\pi b_2\frac{X_2}{L}\right) + C_4\sinh\left(2\pi b_2\frac{X_2}{L}\right)\end{array}\right]\\
\Delta U_2 &= \cos\left(2\pi\frac{X_1}{L}\right)\\
&\left[\begin{array}{l} N_1C_1\sinh\left(2\pi b_1\frac{X_2}{L}\right) + N_1C_2\cosh\left(2\pi b_1\frac{X_2}{L}\right)\\ +N_2C_3\sinh\left(2\pi b_2\frac{X_2}{L}\right) + N_2C_4\cosh\left(2\pi b_2\frac{X_2}{L}\right)\end{array}\right]
\end{aligned} \tag{53}$$

In Eq. (53), C_1, C_2, C_3, and C_4 are coefficients to be determined. The coefficients b_1, b_2, N_1, N_2 are functions of the dimensionless critical buckling load α. Similar to Eqs. (41)–(43), traction-free condition requires

$$\begin{aligned}
(1-\underline{\alpha})\frac{\partial\Delta U_1}{\partial X_2} + (1+\underline{\bar{\nu}\alpha})\frac{\partial\Delta U_2}{\partial X_1} &= 0\\
(1+\underline{\bar{\nu}\alpha})\frac{\partial\Delta U_2}{\partial X_2} + \bar{\nu}(1-\underline{\alpha})\frac{\partial\Delta U_1}{\partial X_1} &= 0
\end{aligned}, \quad \text{at } X_2 = \pm t \tag{54}$$

which yields

$$\begin{aligned}
&[(1+\underline{\bar{\nu}\alpha})N_1 - (1-\underline{\alpha})b_1]\sinh(b_1kt)C_1 + [(1+\underline{\bar{\nu}\alpha})N_1 - (1-\underline{\alpha})b_1]\cosh(b_1kt)C_2\\
&+ [(1+\underline{\bar{\nu}\alpha})N_2 - (1-\underline{\alpha})b_2]\sinh(b_2kt)C_3 + [(1+\underline{\bar{\nu}\alpha})N_2 - (1-\underline{\alpha})b_2]\cosh(b_2kt)C_4 = 0\\
&[(1+\underline{\bar{\nu}\alpha})N_1b_1 + (1-\underline{\alpha})\bar{\nu}]\cosh(b_1kt)C_1 + [(1+\underline{\bar{\nu}\alpha})N_1b_1 + (1-\underline{\alpha})\bar{\nu}]\sinh(b_1kt)C_2\\
&+ [(1+\underline{\bar{\nu}\alpha})N_2b_2 + (1-\underline{\alpha})\bar{\nu}]\cosh(b_2kt)C_3 + [(1+\underline{\bar{\nu}\alpha})N_2b_2 + (1-\underline{\alpha})\bar{\nu}]\sinh(b_2kt)C_4 = 0\\
&[(1+\underline{\bar{\nu}\alpha})N_1 - (1-\underline{\alpha})b_1]\sinh(b_1kt)C_1 - [(1+\underline{\bar{\nu}\alpha})N_1 - (1-\underline{\alpha})b_1]\cosh(b_1kt)C_2\\
&+ [(1+\underline{\bar{\nu}\alpha})N_2 - (1-\underline{\alpha})b_2]\sinh(b_2kt)C_3 - [(1+\underline{\bar{\nu}\alpha})N_2 - (1-\underline{\alpha})b_2]\cosh(b_2kt)C_4 = 0\\
&[(1+\underline{\bar{\nu}\alpha})N_1b_1 + (1-\underline{\alpha})\bar{\nu}]\cosh(b_1kt)C_1 - [(1+\underline{\bar{\nu}\alpha})N_1b_1 + (1-\underline{\alpha})\bar{\nu}]\sinh(b_1kt)C_2\\
&+ [(1+\underline{\bar{\nu}\alpha})N_2b_2 + (1-\underline{\alpha})\bar{\nu}]\cosh(b_2kt)C_3 - [(1+\underline{\bar{\nu}\alpha})N_2b_2 + (1-\underline{\alpha})\bar{\nu}]\sinh(b_2kt)C_4 = 0
\end{aligned} \tag{55}$$

The determinant M of the coefficient matrix of Eq. (55) must be zero for nontrivial solution, which yields the dimensionless critical buckling load α. Here, it can be shown that

$$M = 4M_1 \cdot M_2 = 0 \tag{56}$$

where

$$\begin{aligned}
\mathrm{M}_1 &= \begin{vmatrix} [(1+\underline{\bar{\nu}\alpha})N_2b_2 + (1-\underline{\alpha})\bar{\nu}]\cosh(b_1kt) & [(1+\underline{\bar{\nu}\alpha})N_1b_1 + (1-\underline{\alpha})\bar{\nu}]\cosh(b_2kt)\\ [(1+\underline{\bar{\nu}\alpha})N_2 - (1-\underline{\alpha})b_2]\sinh(b_1kt) & [(1+\underline{\bar{\nu}\alpha})N_1 - (1-\underline{\alpha})b_1]\sinh(b_2kt)\end{vmatrix}\\
\mathrm{M}_2 &= \begin{vmatrix} [(1+\underline{\bar{\nu}\alpha})N_2 - (1-\underline{\alpha})b_2]\sinh(b_2kt) & [(1+\underline{\bar{\nu}\alpha})N_1 - (1-\underline{\alpha})b_1]\sinh(b_1kt)\\ [(1+\underline{\bar{\nu}\alpha})N_2b_2 + (1-\underline{\alpha})\bar{\nu}]\cosh(b_2kt) & [(1+\underline{\bar{\nu}\alpha})N_1b_1 + (1-\underline{\alpha})\bar{\nu}]\cosh(b_1kt)\end{vmatrix}
\end{aligned} \tag{57}$$

The condition $\mathrm{M}_1 = 0$ gives the lowest critical buckling load, which can be obtained from the following equation

$$\begin{aligned}
&[(1+\underline{\bar{\nu}\alpha})N_1b_1 + (1-\underline{\alpha})\bar{\nu}][(1+\underline{\bar{\nu}\alpha})N_2 - (1-\underline{\alpha})b_2]\tanh\left(2\pi b_1\frac{t}{L}\right)\\
&- [(1+\underline{\bar{\nu}\alpha})N_2b_2 + (1-\underline{\alpha})\bar{\nu}][(1+\underline{\bar{\nu}\alpha})N_1 - (1-\underline{\alpha})b_1]\tanh\left(2\pi b_2\frac{t}{L}\right) = 0
\end{aligned} \tag{58}$$

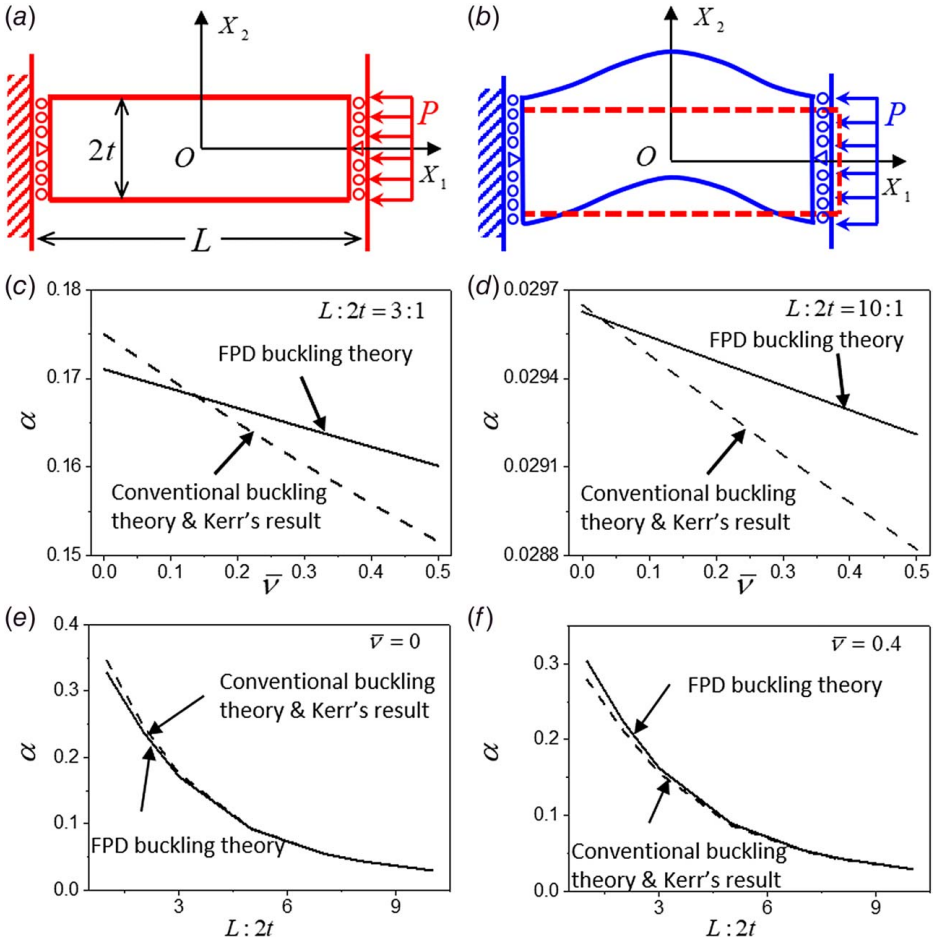

Fig. 3 Buckling analysis of the elastic rectangular solid with the constitutive model $\boldsymbol{T=L:E}$. The (*a*) undeformed and (*b*) buckling modes. The curves of the dimensionless critical buckling load α versus the Poisson's ratio $\bar{\nu}$ for (c) $L:2t=3:1$ and (*d*) $L:2t=10:1$. The curves of the dimensionless critical buckling load α versus the aspect ratio $L:2t$ for (e) $\bar{\nu}=0$ and (*f*) $\bar{\nu}=0.4$.

Without the consideration of the prebuckling deformation before the onset of buckling (CBT), Eq. (58) becomes

$$(N_1b_1+\bar{\nu})(N_2-b_2)\tanh\left(2\pi b_1\frac{t}{L}\right) - (N_2b_2+\bar{\nu})(N_1-b_1)\tanh\left(2\pi b_2\frac{t}{L}\right)=0 \tag{59}$$

which agrees well with the results by Timoshenko and Gere [7] and Kerr and Tang [19].

For cases which justify the assumption of slender beams

$$\alpha \ll 1 \text{ and } \frac{t}{L}\ll 1 \tag{60}$$

both Eqs. (58) and (59) can be simplified and yield

$$\alpha=\frac{\pi^2(2t)^2}{3L^2} \tag{61}$$

which agrees well with the classic solution of Euler buckling.

The aspect ratio L: $2t$ and the Poisson's ratio $\bar{\nu}$ are the only two parameters for the buckling analysis of the elastic rectangular solid. Figures 3(*c*)–3(*f*) show the comparison of the dimensionless critical buckling load α by the FPD buckling theory and the CBT. The solid line shows the result from Eq. (58) by FPD buckling theory, while the dashed line gives the result from Eq. (59) by the CBT without the consideration of the effects of finite prebuckling deformation, which is consistent with the results by Kerr and Tang [19]. Similar to the buckling of the elastic semi-plane solid, the dimensionless critical buckling load α decreases with the increase of the Poisson's ratio $\bar{\nu}$ (Figs. 3(*c*) and 3(*d*)). For L: $2t=3:1$, the maximum error yielded by the neglect of the finite prebuckling deformation is about 6% (Fig. 3(*c*)), which occurs at $\bar{\nu}\to 0.5$. For larger aspect ratio (Fig. 3(*d*)), e.g., L: $2t=10:1$, the elastic rectangular solid approaches the Euler beam and the error becomes very small, as indicated in the analytic derivation of Eqs. (58)–(61). Figures 3(*e*) and 3(*f*) show the effects of the aspect ratio L: $2t$ with $\bar{\nu}\to 0$ and $\bar{\nu}\to 0.4$, respectively. For L: $2t\le 3:1$, the error yielded by the neglect of the finite prebuckling deformation is considerable, while for large aspect ratio, both results by FPD buckling theory and the CBT approach the Euler buckling.

4 Examples With the Constitutive Model $\overset{\nabla}{\boldsymbol{\tau}}=\boldsymbol{L}:\boldsymbol{d}$

4.1 The Analysis of the Constitutive Model. Another widely used constitutive model is that the Janmann rate of the Kirchhoff stress $\boldsymbol{\tau}$, i.e.

$$\overset{\nabla}{\boldsymbol{\tau}}=\dot{\boldsymbol{\tau}}-\boldsymbol{w}\cdot\boldsymbol{\tau}+\boldsymbol{\tau}\cdot\boldsymbol{w} \tag{62}$$

is linearly proportional to the deformation rate $\boldsymbol{d}$

$$\overset{\nabla}{\boldsymbol{\tau}}=\boldsymbol{L}:\boldsymbol{d} \tag{63}$$

where $\boldsymbol{w}$ is the spin rate. Equation (63) should be converted to the expression in terms of the second Piola-Kirchhoff stress $\boldsymbol{T}$ and the

Green strain $\boldsymbol{E}$, for the convenience of the derivation here. According to the relations among different types of stresses and strains (or stress and strain rates)

$$\boldsymbol{\tau} = \boldsymbol{F} \cdot \boldsymbol{T} \cdot \boldsymbol{F}^T \tag{64}$$

and

$$\boldsymbol{d} = \boldsymbol{F}^{-T} \cdot \dot{\boldsymbol{E}} \cdot \boldsymbol{F}^{-1} \tag{65}$$

Equation (63) is converted to

$$\dot{\boldsymbol{T}} = [(\boldsymbol{F}^{-1}\boldsymbol{F}^{-1}\boldsymbol{F}^{-1}\boldsymbol{F}^{-1})^{*}_{*}\boldsymbol{L}]:\dot{\boldsymbol{E}} - \boldsymbol{F}^{-1} \cdot \boldsymbol{F}^{-T} \cdot \dot{\boldsymbol{E}} \cdot \boldsymbol{T} - \boldsymbol{T} \cdot \dot{\boldsymbol{E}} \cdot \boldsymbol{F}^{-1} \cdot \boldsymbol{F}^{-T} \tag{66}$$

According to the rule of derivation for FPD buckling theory, constitutive model (66) can be simplified to

$$\Delta\boldsymbol{T} = \left[\left(\overset{\circ}{\boldsymbol{F}}{}^{-1}\overset{\circ}{\boldsymbol{F}}{}^{-1}\overset{\circ}{\boldsymbol{F}}{}^{-1}\overset{\circ}{\boldsymbol{F}}{}^{-1}\right)^{*}_{*}\boldsymbol{L}\right]:\Delta\boldsymbol{E} - \overset{\circ}{\boldsymbol{F}}{}^{-1} \cdot \overset{\circ}{\boldsymbol{F}}{}^{-T} \cdot \Delta\boldsymbol{E} \cdot \overset{\circ}{\boldsymbol{T}} - \overset{\circ}{\boldsymbol{T}} \cdot \Delta\boldsymbol{E} \cdot \overset{\circ}{\boldsymbol{F}}{}^{-1} \cdot \overset{\circ}{\boldsymbol{F}}{}^{-T} \tag{67}$$

For uniaxial compression, only stress $\overset{\circ}{T}_{11}$ is nonzero before the onset of buckling as shown in Eq. (27). The deformation gradient before the onset of buckling is

$$\begin{aligned}
\overset{\circ}{\boldsymbol{F}} &= \left(1 + \frac{\partial \overset{\circ}{U}_1}{\partial X_1}\right)\boldsymbol{E}_1\boldsymbol{E}_1 + \left(1 + \frac{\partial \overset{\circ}{U}_2}{\partial X_2}\right)\boldsymbol{E}_2\boldsymbol{E}_2 \\
\overset{\circ}{\boldsymbol{F}}{}^{-1} &= \left(1 - \frac{\partial \overset{\circ}{U}_1}{\partial X_1}\right)\boldsymbol{E}_1\boldsymbol{E}_1 + \left(1 - \frac{\partial \overset{\circ}{U}_2}{\partial X_2}\right)\boldsymbol{E}_2\boldsymbol{E}_2 + \cdots \\
\overset{\circ}{\boldsymbol{F}}{}^{-T} &= \left(1 - \frac{\partial \overset{\circ}{U}_1}{\partial X_1}\right)\boldsymbol{E}_1\boldsymbol{E}_1 + \left(1 - \frac{\partial \overset{\circ}{U}_2}{\partial X_2}\right)\boldsymbol{E}_2\boldsymbol{E}_2 + \cdots
\end{aligned} \tag{68}$$

Substitution of Eqs. (27) and (68) into Eq. (67) yields the expanded constitutive model for the critical buckling analysis

$$\begin{aligned}
\Delta T_{11} &= \frac{\overline{E}}{1-\bar{\nu}^2}\left[\left(1 - 4\frac{\partial \overset{\circ}{U}_1}{\partial X_1}\right)\Delta E_{11} + \left(1 - 2\frac{\partial \overset{\circ}{U}_1}{\partial X_1} - 2\frac{\partial \overset{\circ}{U}_2}{\partial X_2}\right)\bar{\nu}\Delta E_{22}\right] \\
&\quad - 2\left(1 - 2\frac{\partial \overset{\circ}{U}_1}{\partial X_1}\right)\overset{\circ}{T}_{11}\Delta E_{11} \\
\Delta T_{22} &= \frac{\overline{E}}{1-\bar{\nu}^2}\left[\left(1 - 4\frac{\partial \overset{\circ}{U}_2}{\partial X_2}\right)\Delta E_{22} + \left(1 - 2\frac{\partial \overset{\circ}{U}_1}{\partial X_1} - 2\frac{\partial \overset{\circ}{U}_2}{\partial X_2}\right)\bar{\nu}\Delta E_{11}\right] \\
\Delta T_{12} &= \Delta T_{21} = \frac{\overline{E}}{1+\bar{\nu}}\left(1 - 2\frac{\partial \overset{\circ}{U}_1}{\partial X_1} - 2\frac{\partial \overset{\circ}{U}_2}{\partial X_2}\right)\Delta E_{12} - \left(1 - 2\frac{\partial \overset{\circ}{U}_2}{\partial X_2}\right)\overset{\circ}{T}_{11}\Delta E_{12}
\end{aligned} \tag{69}$$

which will be used in the following examples.

4.2 Buckling of an Elastic Semi-Plane Solid Subject to Compression. The solving process for buckling of an elastic semi-plane solid subject to compression is the same with Sec. 3.1. Substitution of the constitutive model Eq. (69) into the equilibrium relations Eq. (29) yields

$$\begin{aligned}
&\frac{\overline{E}}{1-\bar{\nu}^2}\frac{\partial}{\partial X_1}\left[\left(1 - 3\frac{\partial \overset{\circ}{U}_1}{\partial X_1}\right)\frac{\partial \Delta U_1}{\partial X_1} + \left(1 - 2\frac{\partial \overset{\circ}{U}_1}{\partial X_1} - \frac{\partial \overset{\circ}{U}_2}{\partial X_2}\right)\bar{\nu}\frac{\partial \Delta U_2}{\partial X_2}\right] \\
&\quad + \frac{\overline{E}}{1+\bar{\nu}}\frac{\partial}{\partial X_2}\frac{1}{2}\left[\left(1 - \frac{\partial \overset{\circ}{U}_1}{\partial X_1} - 2\frac{\partial \overset{\circ}{U}_2}{\partial X_2}\right)\frac{\partial \Delta U_1}{\partial X_2} + \left(1 - 2\frac{\partial \overset{\circ}{U}_1}{\partial X_1} - \frac{\partial \overset{\circ}{U}_2}{\partial X_2}\right)\frac{\partial \Delta U_2}{\partial X_1}\right] \\
&\quad + P\left\{\frac{\partial}{\partial X_1}\left(1 - \frac{\partial \overset{\circ}{U}_1}{\partial X_1}\right)\frac{\partial \Delta U_1}{\partial X_1} + \frac{\partial}{\partial X_2}\frac{1}{2}\left[\left(1 - 2\frac{\partial \overset{\circ}{U}_2}{\partial X_2} + \frac{\partial \overset{\circ}{U}_1}{\partial X_1}\right)\frac{\partial \Delta U_1}{\partial X_2} + \left(1 - \frac{\partial \overset{\circ}{U}_2}{\partial X_2}\right)\frac{\partial \Delta U_2}{\partial X_1}\right]\right\} = 0 \\
&\quad \frac{\overline{E}}{1+\bar{\nu}}\frac{\partial}{\partial X_1}\frac{1}{2}\left[\left(1 - \frac{\partial \overset{\circ}{U}_1}{\partial X_1} - 2\frac{\partial \overset{\circ}{U}_2}{\partial X_2}\right)\frac{\partial \Delta U_1}{\partial X_2} + \left(1 - 2\frac{\partial \overset{\circ}{U}_1}{\partial X_1} - \frac{\partial \overset{\circ}{U}_2}{\partial X_2}\right)\frac{\partial \Delta U_2}{\partial X_1}\right] \\
&\quad + \frac{\overline{E}}{1-\bar{\nu}^2}\frac{\partial}{\partial X_2}\left[\left(1 - 3\frac{\partial \overset{\circ}{U}_2}{\partial X_2}\right)\frac{\partial \Delta U_2}{\partial X_2} + \left(1 - \frac{\partial \overset{\circ}{U}_1}{\partial X_1} - 2\frac{\partial \overset{\circ}{U}_2}{\partial X_2}\right)\bar{\nu}\frac{\partial \Delta U_1}{\partial X_1}\right] \\
&\quad + P\frac{\partial}{\partial X_1}\frac{1}{2}\left[\left(1 + \frac{\partial \overset{\circ}{U}_1}{\partial X_1} - 2\frac{\partial \overset{\circ}{U}_2}{\partial X_2}\right)\frac{\partial \Delta U_1}{\partial X_2} - \left(1 - \frac{\partial \overset{\circ}{U}_2}{\partial X_2}\right)\frac{\partial \Delta U_2}{\partial X_1}\right] = 0
\end{aligned} \tag{70}$$

The underlined terms in Eq. (70) are for the effects of the prebuckling deformation while the prebuckling stress/force P is the critical buckling load to be obtained. Using the definition of dimensionless critical buckling load $\alpha = P/\overline{E}$, Eq. (70) becomes

$$\begin{aligned}
&[1 + 3\underline{\alpha} + \alpha(1-\bar{\nu}^2)]\frac{\partial^2 \Delta U_1}{\partial X_1^2} + \frac{1}{2}[(1 + \underline{\alpha - 2\bar{\nu}\alpha})(1-\bar{\nu}) + \alpha(1-\bar{\nu}^2)] \\
&\quad \frac{\partial^2 \Delta U_1}{\partial X_2^2} + \frac{1}{2}[(1 + \underline{2\alpha - \bar{\nu}\alpha})(1+\bar{\nu}) + \alpha(1-\bar{\nu}^2)]\frac{\partial^2 \Delta U_2}{\partial X_1 \partial X_2} = 0 \\
&\quad (1 - \underline{3\bar{\nu}\alpha})\frac{\partial^2 \Delta U_2}{\partial X_2^2} + \frac{1}{2}[(1 + \underline{2\alpha - \bar{\nu}\alpha})(1-\bar{\nu}) - \alpha(1-\bar{\nu}^2)]\frac{\partial^2 \Delta U_2}{\partial X_1^2} \\
&\quad + \frac{1}{2}[(1 + \underline{\alpha - 2\bar{\nu}\alpha})(1+\bar{\nu}) + \alpha(1-\bar{\nu}^2)]\frac{\partial^2 \Delta U_1}{\partial X_1 \partial X_2} = 0
\end{aligned} \tag{71}$$

Equation (71) is the same type equation with Eq. (33), but with different coefficients. The general solution (34) and the relations (36) also work for Eq. (71). The coefficients b_1, b_2, N_1, and N_2 in Eqs. (35) and (37) become

$$b_1 = \sqrt{\frac{\left\{\begin{array}{l} -(\bar{\nu}+1)^2(\bar{\nu}-1)^2\alpha^2 + (\bar{\nu}+1)(\bar{\nu}-1)^2\alpha - 2\bar{\nu} + 2 \\ \underline{+(-\bar{\nu}^4 + 2\bar{\nu}^3 + 12\bar{\nu}^2 - 28\bar{\nu} - 1)\alpha^2 + 6(\bar{\nu}-1)^2\alpha} \\ + \sqrt{(\bar{\nu}+1)^3\alpha^2\left[\begin{array}{l} (\bar{\nu}+1)(\bar{\nu}-1)^2(\alpha\bar{\nu} - \alpha - 1)^2 \\ \underline{+(3\bar{\nu}^5 - 41\bar{\nu}^4 + 174\bar{\nu}^3 - 306\bar{\nu}^2 + 199\bar{\nu} + 3)\alpha^2} \\ \underline{-2(\bar{\nu}^2 - 16\bar{\nu} + 31)(\bar{\nu}-1)^2\alpha - 8(\bar{\nu}-1)(\bar{\nu}-2)} \end{array}\right]} \end{array}\right\}}{2(1-\bar{\nu})[\bar{\nu}\alpha + \alpha + 1 + \underline{(3\bar{\nu}^2 - 6\bar{\nu})\alpha^2 + (1-5\bar{\nu})\alpha}]}} \tag{72}$$

$$b_2 = \sqrt{\frac{\left\{\begin{array}{l} -(\bar{\nu}+1)^2(\bar{\nu}-1)^2\alpha^2 + (\bar{\nu}+1)(\bar{\nu}-1)^2\alpha - 2\bar{\nu} + 2 \\ \underline{+(-\bar{\nu}^4 + 2\bar{\nu}^3 + 12\bar{\nu}^2 - 28\bar{\nu} - 1)\alpha^2 + 6(\bar{\nu}-1)^2\alpha} \\ - \sqrt{(\bar{\nu}+1)^3\alpha^2\left[\begin{array}{l} (\bar{\nu}+1)(\bar{\nu}-1)^2(\alpha\bar{\nu} - \alpha - 1)^2 \\ \underline{+(3\bar{\nu}^5 - 41\bar{\nu}^4 + 174\bar{\nu}^3 - 306\bar{\nu}^2 + 199\bar{\nu} + 3)\alpha^2} \\ \underline{-2(\bar{\nu}^2 - 16\bar{\nu} + 31)(\bar{\nu}-1)^2\alpha - 8(\bar{\nu}-1)(\bar{\nu}-2)} \end{array}\right]} \end{array}\right\}}{2(1-\bar{\nu})[\bar{\nu}\alpha + \alpha + 1 + \underline{(3\bar{\nu}^2 - 6\bar{\nu})\alpha^2 + (1-5\bar{\nu})\alpha}]}}$$

and

$$\begin{aligned} N_1 &= \frac{b_1(\bar{\nu}+1)(\bar{\nu}\alpha - \alpha - 1 + \underline{2\bar{\nu}\alpha - \alpha})}{(1-\bar{\nu}^2)\alpha + 2b_1^2 + \bar{\nu} - 1\underline{+(-6\bar{\nu}b_1^2 - \bar{\nu}^2 + 3\bar{\nu} - 2)\alpha}} \\ N_2 &= \frac{b_2(\bar{\nu}+1)(\bar{\nu}\alpha - \alpha - 1 + \underline{2\bar{\nu}\alpha - \alpha})}{(1-\bar{\nu}^2)\alpha + 2b_2^2 + \bar{\nu} - 1\underline{+(-6\bar{\nu}b_2^2 - \bar{\nu}^2 + 3\bar{\nu} - 2)\alpha}} \end{aligned} \tag{73}$$

which are functions of the dimensionless critical buckling load α, while $\bar{\nu}$ is the Poisson's ratio. The derivations (38)–(42) also work here. Using Eqs. (22), (69), (27), and (32), Eq. (43) becomes

$$\begin{aligned} &(1 + \underline{\alpha - 2\bar{\nu}\alpha})\frac{\partial \Delta U_1}{\partial X_2} + (1 + \underline{2\alpha - \bar{\nu}\alpha})\frac{\partial \Delta U_2}{\partial X_1} + \alpha(1+\bar{\nu})\left(\frac{\partial \Delta U_1}{\partial X_2} + \frac{\partial \Delta U_2}{\partial X_1}\right) = 0 \\ &(1 - \underline{3\bar{\nu}\alpha})\frac{\partial \Delta U_2}{\partial X_2} + (1 + \underline{\alpha - 2\bar{\nu}\alpha})\bar{\nu}\frac{\partial \Delta U_1}{\partial X_1} = 0 \end{aligned} \quad , \text{ at } X_2 = 0 \tag{74}$$

The solution (40) needs to satisfy the requirements (74), i.e.

$$\begin{bmatrix} \begin{bmatrix} (1 + \underline{2\alpha - \bar{\nu}\alpha} + \alpha + \bar{\nu}\alpha)N_1 \\ -(1 + \underline{\alpha - 2\bar{\nu}\alpha} + \alpha + \bar{\nu}\alpha)b_1 \end{bmatrix} & \begin{bmatrix} (1 + \underline{2\alpha - \bar{\nu}\alpha} + \alpha + \bar{\nu}\alpha)N_2 \\ -(1 + \underline{\alpha - 2\bar{\nu}\alpha} + \alpha + \bar{\nu}\alpha)b_2 \end{bmatrix} \\ (1 - \underline{3\bar{\nu}\alpha})N_1 b_1 + (1 + \underline{\alpha - 2\bar{\nu}\alpha})\bar{\nu} & (1 - \underline{3\bar{\nu}\alpha})N_2 b_2 + (1 + \underline{\alpha - 2\bar{\nu}\alpha})\bar{\nu} \end{bmatrix} \begin{pmatrix} C_1 \\ C_3 \end{pmatrix} = 0 \tag{75}$$

The determinant of the coefficient matrix of Eq. (75) must be zero for nontrivial solution. It requires

$$\begin{aligned} &\begin{bmatrix} (1 + \underline{2\alpha - \bar{\nu}\alpha} + \alpha + \bar{\nu}\alpha)N_1 \\ -(1 + \underline{\alpha - 2\bar{\nu}\alpha} + \alpha + \bar{\nu}\alpha)b_1 \end{bmatrix}[(1 - \underline{3\bar{\nu}\alpha})N_2 b_2 + (1 + \underline{\alpha - 2\bar{\nu}\alpha})\bar{\nu}] \\ &- \begin{bmatrix} (1 + \underline{2\alpha - \bar{\nu}\alpha} + \alpha + \bar{\nu}\alpha)N_2 \\ -(1 + \underline{\alpha - 2\bar{\nu}\alpha} + \alpha + \bar{\nu}\alpha)b_2 \end{bmatrix}[(1 - \underline{3\bar{\nu}\alpha})N_1 b_1 + (1 + \underline{\alpha - 2\bar{\nu}\alpha})\bar{\nu}] = 0 \end{aligned} \tag{76}$$

the solution of which gives the dimensionless critical buckling load α. Similar to the results in Sec. 3.1, there is only one critical buckling load which corresponds to infinite buckling modes for the elastic semi-plane solid.

Without the consideration of the prebuckling deformation (CBT), the equilibrium Eq. (70) and the boundary conditions (74) become

$$\begin{aligned} &\frac{\overline{E}}{1-\bar{\nu}^2}\frac{\partial^2 \Delta U_1}{\partial X_1^2} + \frac{\overline{E}}{2(1+\bar{\nu})}\frac{\partial^2 \Delta U_1}{\partial X_2^2} + \frac{\overline{E}}{2(1-\bar{\nu})}\frac{\partial^2 \Delta U_2}{\partial X_1 \partial X_2} + P\frac{\partial^2 \Delta U_1}{\partial X_1^2} + \frac{P}{2}\left(\frac{\partial^2 \Delta U_1}{\partial X_2^2} + \frac{\partial^2 \Delta U_2}{\partial X_1 \partial X_2}\right) = 0 \\ &\frac{\overline{E}}{1-\bar{\nu}^2}\frac{\partial^2 \Delta U_2}{\partial X_2^2} + \frac{\overline{E}}{2(1+\bar{\nu})}\frac{\partial^2 \Delta U_2}{\partial X_1^2} + \frac{\overline{E}}{2(1-\bar{\nu})}\frac{\partial^2 \Delta U_1}{\partial X_1 \partial X_2} - \frac{P}{2}\left(\frac{\partial^2 \Delta U_2}{\partial X_1^2} - \frac{\partial^2 \Delta U_1}{\partial X_1 \partial X_2}\right) = 0 \end{aligned} \tag{77}$$

and

$$\begin{matrix}\dfrac{\partial \Delta U_1}{\partial X_2}+\dfrac{\partial \Delta U_2}{\partial X_1}=0\\ \dfrac{\partial \Delta U_2}{\partial X_2}+\bar{\nu}\dfrac{\partial \Delta U_1}{\partial X_1}=0\end{matrix},\quad \text{at } X_2=0 \tag{78}$$

The general solution (34) and the relations (36) also work here. The coefficients b_1, b_2, N_1, and N_2 in Eqs. (35) and (37) become

$$b_1=1,\quad b_2=\sqrt{\frac{(\bar{\nu}^2\alpha-\alpha-1)(\bar{\nu}\alpha+\alpha-1)}{(\bar{\nu}\alpha+\alpha+1)}} \tag{79}$$

and

$$N_1=\frac{b_1(\bar{\nu}+1)(\bar{\nu}\alpha-\alpha-1)}{(1-\bar{\nu}^2)\alpha+2b_1^2+\bar{\nu}-1},\quad N_2=\frac{b_2(\bar{\nu}+1)(\bar{\nu}\alpha-\alpha-1)}{(1-\bar{\nu}^2)\alpha+2b_2^2+\bar{\nu}-1} \tag{80}$$

Equation (76) for the dimensionless critical buckling load degenerates to

$$(N_1b_1+\bar{\nu})(N_2-b_2)-(N_2b_2+\bar{\nu})(N_1-b_1)=0 \tag{81}$$

substitution of Eqs. (79) and (80) into which yield the algebraic equation

$$(\bar{\nu}^2+2\bar{\nu}+1)\alpha^3+(2\bar{\nu}+2)\alpha^2-1=0 \tag{82}$$

The solution for the lowest dimensionless critical buckling load is

$$\alpha=\frac{\left(12\sqrt{3(27\bar{\nu}-5)(\bar{\nu}+1)}+108\bar{\nu}+44\right)^{1/3}}{6(\bar{\nu}+1)}+\frac{8}{3(\bar{\nu}+1)\left(12\sqrt{3(27\bar{\nu}-5)(\bar{\nu}+1)}+108\bar{\nu}+44\right)^{1/3}}-\frac{2}{3(\bar{\nu}+1)} \tag{83}$$

It is worth to point out that α is a real number for both $3(27\bar{\nu}-5)(\bar{\nu}+1)\geq 0$ and $3(27\bar{\nu}-5)(\bar{\nu}+1)<0$.

The comparison of results from various methods is shown in Fig. 4(*a*). The solid line shows the dimensionless critical buckling load α by the FPD buckling theory (Eqs. (72), (73), and (76)). It decreases with the increase of the Poisson's ratio. Without the consideration of the effects of the prebuckling deformation (CBT), Eq. (83) gives a significantly reduced α as denoted by the dashed line, which agrees well with the CNM. The disturbing-loading-unloading method (DLU) method [13], the detail of which will be given in the next paragraph, is adopted to obtain the accurate critical buckling load. The predictions of the CBT and the CNM result an unacceptable error (as large as 70% for $\bar{\nu}=0$), while our FPD buckling theory can give a better result (the error decreases to 20% for $\bar{\nu}=0$). It is obvious that the prebuckling deformation becomes significantly important and nonnegligible. Nevertheless, the critical buckling load obtained by FPD buckling theory approaches to the CBT and the CNM result with the increasing Poisson's ratio and results in an inaccuracy as large as 58% for $\bar{\nu}=0.5$. The inaccuracy is because that the DLU method is a nonlinear analysis which is powerful to accurately capture the mechanical behavior of structures with the consideration of both prebuckling stress and deformation, while in the FPD buckling theory, the prebuckling analysis is accurate to the first power of displacements for all the components.

The disturbing-loading-unloading (DLU) method, which is valid only for simple elastic structures, is first developed for the investigation of the FPD behaviors of 3D beams [13]. For the elastic semi-plane solid, two curves of compression stress versus compression strain are obtained, as shown in Fig. 4(*b*) for $\bar{\nu}=0.5$, i.e., the curve for nonbuckling (uniform compression) and the curve for the real deformation mode with both nonbuckling at the beginning and buckling at the following. By the comparison of the two curves, the critical buckling load is obtained at the bifurcation, beyond which the applied compression stress and the elastic energy in the buckling regime are lower than those in the nonbuckling regime. The real buckling point is far beyond that obtained by the CNM and CBT.

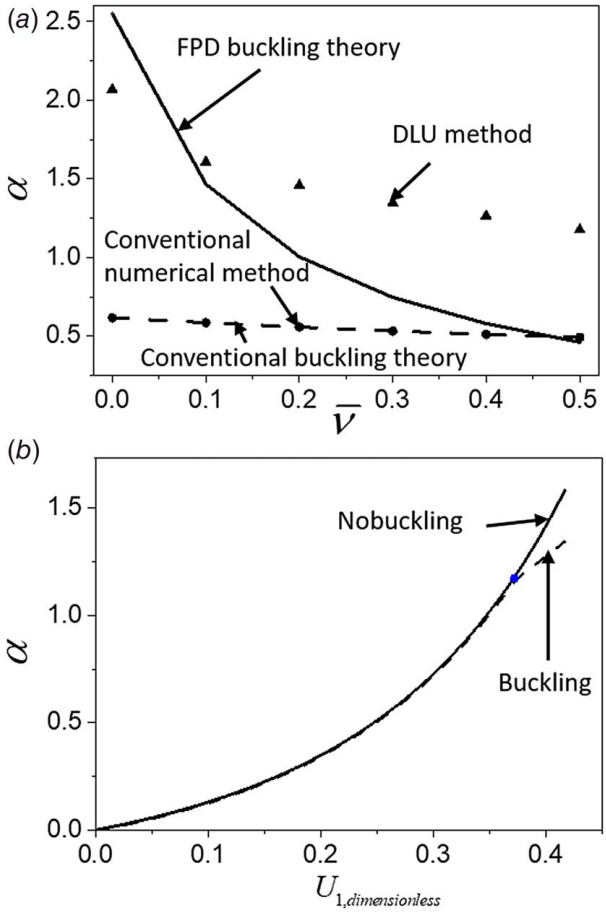

Fig. 4 Buckling analysis of the elastic semi-plane solid with the constitutive model $\tau=L:d$. (*a*) The curves of the dimensionless critical buckling load α versus the Poisson's ratio $\bar{\nu}$ for the FPD buckling theory, the CBT, the CNM, and the DLU method and (*b*) Compress stress–strain curves for nonbuckling (uniform compression) and the real deformation mode with both nonbuckling at the beginning and buckling at the following.

4.3 Buckling of an Elastic Rectangular Solid Subject to Compression. For the buckling of a rectangular elastic solid subject to compression, the derivation from Eqs. (51) to (53) also work here, but the coefficients b_1, b_2, N_1, N_2 become the expression given in Eqs. (72) and (73). The Eqs. (54), (55), (57), and (58) become

$$\begin{aligned}&(1+\underline{\alpha-2\bar{\nu}\alpha})\frac{\partial \Delta U_1}{\partial X_2}+(1+\underline{2\alpha-\bar{\nu}\alpha})\frac{\partial \Delta U_2}{\partial X_1}\\&+\alpha(1+\bar{\nu})\left(\frac{\partial \Delta U_1}{\partial X_2}+\frac{\partial \Delta U_2}{\partial X_1}\right)=0(1-\underline{3\bar{\nu}\alpha})\frac{\partial \Delta U_2}{\partial X_2}\\&+(1+\underline{\alpha-2\bar{\nu}\alpha})\bar{\nu}\frac{\partial \Delta U_1}{\partial X_1}=0,\quad \text{at } X_2=\pm t,\end{aligned} \tag{84}$$

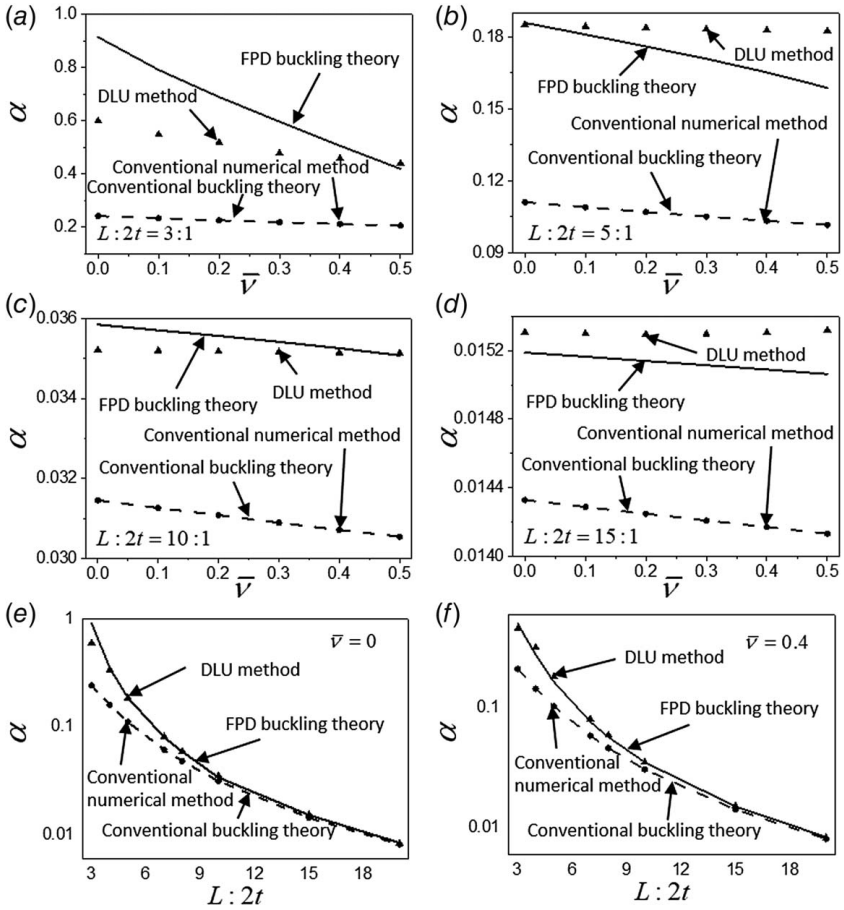

Fig. 5 Buckling analysis of the elastic rectangular solid with the constitutive model $\overset{\nabla}{\tau} = L{:}d$. The curves of the dimensionless critical buckling load α versus the Poisson's ratio $\bar{\nu}$ for (*a*) $L{:}2t = 3{:}1$, (*b*) $L{:}2t = 5{:}1$, (*c*) $L{:}2t = 10{:}1$, and (*d*) $L{:}2t = 15{:}1$. The curves of the dimensionless critical buckling load α versus the aspect ratio $L{:}2t$ for (*e*) $\bar{\nu} = 0$ and (*f*) $\bar{\nu} = 0.4$.

$$
\begin{bmatrix} (1+\underline{2\alpha-\bar{\nu}\alpha}+\alpha+\bar{\nu}\alpha)N_1 \\ -(1+\underline{\alpha-2\bar{\nu}\alpha}+\alpha+\bar{\nu}\alpha)b_1 \end{bmatrix}\sinh(b_1kt)C_1 + \begin{bmatrix} (1+\underline{2\alpha-\bar{\nu}\alpha}+\alpha+\bar{\nu}\alpha)N_1 \\ -(1+\underline{\alpha-2\bar{\nu}\alpha}+\alpha+\bar{\nu}\alpha)b_1 \end{bmatrix}\cosh(b_1kt)C_2
$$
$$
+ \begin{bmatrix} (1+\underline{2\alpha-\bar{\nu}\alpha}+\alpha+\bar{\nu}\alpha)N_2 \\ -(1+\underline{\alpha-2\bar{\nu}\alpha}+\alpha+\bar{\nu}\alpha)b_2 \end{bmatrix}\sinh(b_2kt)C_3 + \begin{bmatrix} (1+\underline{2\alpha-\bar{\nu}\alpha}+\alpha+\bar{\nu}\alpha)N_2 \\ -(1+\underline{\alpha-2\bar{\nu}\alpha}+\alpha+\bar{\nu}\alpha)b_2 \end{bmatrix}\cosh(b_2kt)C_4 = 0
$$
$$
[(1-\underline{3\bar{\nu}\alpha})N_1b_1 + (1+\underline{\alpha-2\bar{\nu}\alpha})\bar{\nu}]\cosh(b_1kt)C_1 + [(1-\underline{3\bar{\nu}\alpha})N_1b_1 + (1+\underline{\alpha-2\bar{\nu}\alpha})\bar{\nu}]\sinh(b_1kt)C_2
$$
$$
+ [(1-\underline{3\bar{\nu}\alpha})N_2b_2 + (1+\underline{\alpha-2\bar{\nu}\alpha})\bar{\nu}]\cosh(b_2kt)C_3 + [(1-\underline{3\bar{\nu}\alpha})N_2b_2 + (1+\underline{\alpha-2\bar{\nu}\alpha})\bar{\nu}]\sinh(b_2kt)C_4 = 0
$$
$$
\begin{bmatrix} (1+\underline{2\alpha-\bar{\nu}\alpha}+\alpha+\bar{\nu}\alpha)N_1 \\ -(1+\underline{\alpha-2\bar{\nu}\alpha}+\alpha+\bar{\nu}\alpha)b_1 \end{bmatrix}\sinh(b_1kt)C_1 - \begin{bmatrix} (1+\underline{2\alpha-\bar{\nu}\alpha}+\alpha+\bar{\nu}\alpha)N_1 \\ -(1+\underline{\alpha-2\bar{\nu}\alpha}+\alpha+\bar{\nu}\alpha)b_1 \end{bmatrix}\cosh(b_1kt)C_2
$$
$$
+ \begin{bmatrix} (1+\underline{2\alpha-\bar{\nu}\alpha}+\alpha+\bar{\nu}\alpha)N_2 \\ -(1+\underline{\alpha-2\bar{\nu}\alpha}+\alpha+\bar{\nu}\alpha)b_2 \end{bmatrix}\sinh(b_2kt)C_3 - \begin{bmatrix} (1+\underline{2\alpha-\bar{\nu}\alpha}+\alpha+\bar{\nu}\alpha)N_2 \\ -(1+\underline{\alpha-2\bar{\nu}\alpha}+\alpha+\bar{\nu}\alpha)b_2 \end{bmatrix}\cosh(b_2kt)C_4 = 0
$$
$$
[(1-\underline{3\bar{\nu}\alpha})N_1b_1 + (1+\underline{\alpha-2\bar{\nu}\alpha})\bar{\nu}]\cosh(b_1kt)C_1 - [(1-\underline{3\bar{\nu}\alpha})N_1b_1 + (1+\underline{\alpha-2\bar{\nu}\alpha})\bar{\nu}]\sinh(b_1kt)C_2
$$
$$
+ [(1-\underline{3\bar{\nu}\alpha})N_2b_2 + (1+\underline{\alpha-2\bar{\nu}\alpha})\bar{\nu}]\cosh(b_2kt)C_3 - [(1-\underline{3\bar{\nu}\alpha})N_2b_2 + (1+\underline{\alpha-2\bar{\nu}\alpha})\bar{\nu}]\sinh(b_2kt)C_4 = 0
$$

(85)

$$
\mathrm{M}_1 = \begin{vmatrix} [(1-\underline{3\bar{\nu}\alpha})N_2b_2 + (1+\underline{\alpha-2\bar{\nu}\alpha})\bar{\nu}]\sinh(b_2kt) & [(1-\underline{3\bar{\nu}\alpha})N_1b_1 + (1+\underline{\alpha-2\bar{\nu}\alpha})\bar{\nu}]\sinh(b_1kt) \\ \begin{bmatrix} (1+\underline{2\alpha-\bar{\nu}\alpha}+\alpha+\bar{\nu}\alpha)N_2 \\ -(1+\underline{\alpha-2\bar{\nu}\alpha}+\alpha+\bar{\nu}\alpha)b_2 \end{bmatrix}\cosh(b_2kt) & \begin{bmatrix} (1+\underline{2\alpha-\bar{\nu}\alpha}+\alpha+\bar{\nu}\alpha)N_1 \\ -(1+\underline{\alpha-2\bar{\nu}\alpha}+\alpha+\bar{\nu}\alpha)b_1 \end{bmatrix}\cosh(b_1kt) \end{vmatrix}
$$
$$
\mathrm{M}_2 = \begin{vmatrix} \begin{bmatrix} (1+\underline{2\alpha-\bar{\nu}\alpha}+\alpha+\bar{\nu}\alpha)N_2 \\ -(1+\underline{\alpha-2\bar{\nu}\alpha}+\alpha+\bar{\nu}\alpha)b_2 \end{bmatrix}\sinh(b_2kt) & \begin{bmatrix} (1+\underline{2\alpha-\bar{\nu}\alpha}+\alpha+\bar{\nu}\alpha)N_1 \\ -(1+\underline{\alpha-2\bar{\nu}\alpha}+\alpha+\bar{\nu}\alpha)b_1 \end{bmatrix}\sinh(b_1kt) \\ [(1-\underline{3\bar{\nu}\alpha})N_2b_2 + (1+\underline{\alpha-2\bar{\nu}\alpha})\bar{\nu}]\cosh(b_2kt) & [(1-\underline{3\bar{\nu}\alpha})N_1b_1 + (1+\underline{\alpha-2\bar{\nu}\alpha})\bar{\nu}]\cosh(b_1kt) \end{vmatrix}
$$

(86)

and

$$[(1-\underline{3\bar{\nu}\alpha})N_1b_1+(1+\underline{\alpha-2\bar{\nu}\alpha})\bar{\nu}]\begin{bmatrix}(1+\underline{2\alpha-\bar{\nu}\alpha}+\alpha+\bar{\nu}\alpha)N_2\\-(1+\underline{\alpha-2\bar{\nu}\alpha}+\alpha+\bar{\nu}\alpha)b_2\end{bmatrix}\tanh\left(2\pi b_1\frac{t}{L}\right)-$$
$$[(1-\underline{3\bar{\nu}\alpha})N_2b_2+(1+\underline{\alpha-2\bar{\nu}\alpha})\bar{\nu}]\begin{bmatrix}(1+\underline{2\alpha-\bar{\nu}\alpha}+\alpha+\bar{\nu}\alpha)N_1\\-(1+\underline{\alpha-2\bar{\nu}\alpha}+\alpha+\bar{\nu}\alpha)b_1\end{bmatrix}\tanh\left(2\pi b_2\frac{t}{L}\right)=0, \quad (87)$$

respectively. From Eq. (87), the exact solution for the dimensionless critical buckling load can be obtained.

Equation (59) holds here for the case without the consideration of finite prebuckling deformation. The coefficients b_1, b_2, N_1, N_2 can be found from Eqs. (72) and (73).

For cases which justify the assumption of the slender beams

$$\alpha \ll 1 \text{ and } \frac{t}{L} \ll 1 \quad (88)$$

Both Eqs. (87) and (59) can be simplified and yield

$$\alpha = \frac{\pi^2(2t)^2}{3L^2} \quad (89)$$

which agrees well with the classic solution of Euler buckling.

Figure 5 shows the comparison of the dimensionless critical buckling load α obtained by various methods. For L: $2t = 3{:}1$, the consistent result from the CNM and the CBT can yield more than 50% error compared with the accurate solution by the DLU method, while the FPD buckling theory is able to give a better prediction (the inaccuracy of the FPD decreases from 50% for $\bar{\nu} = 0$ to 5% for $\bar{\nu} = 0.5$). For larger aspect ratio L: $2t = 5{:}1$, 10:1, and 15:1, the elastic rectangular solid approaches the Euler beam and the error becomes very small, as indicated Figs. 5(*b*)–5(*d*), respectively. However, the result obtained by FPD buckling theory is always closer, than that of the CNM and the CBT, to the accurate solution by the DLU method. Figures 5(*e*) and 5(*f*) give the curves of the dimensionless critical buckling load and the aspect ratio and confirm the above analysis. The result of all the four methods approaches that of the Euler buckling.

5 Discussion and Concluding Remarks

(i) In the conventional buckling problems, the prebuckling deformation is usually very small and is neglected in most of the CBT and CNM. In this paper, we find that the FPD buckling behaviors also exist in bulk structures, while we have focused on that of 3D beams in the preceding paper [13].

(ii) On the basis of the theory of the finite deformation, a systematic and straightforward FPD buckling theory is developed for bulk structures by considering the effects of finite prebuckling deformation. It accounts for all terms up to the first power of displacement (with "Δ") in the deformation components for critical buckling analysis, and the variables with "o", serve as the coefficients of the incremental terms, also accurate to the first power.

(iii) Two constitutive models including the Saint-Venant-Kirchhoff model, which is $\boldsymbol{T}=\boldsymbol{L}:\boldsymbol{E}$ and $\overset{\nabla}{\boldsymbol{\tau}}=\boldsymbol{L}:\boldsymbol{d}$ are adopted in the FPD buckling analysis, and give much different results.

(iv) Four methods, including the CBT, CNM, DLU method, and FPD buckling theory, are applied to the classic problems, including buckling of an elastic semi-plane solid and buckling of an elastic rectangular solid, respectively. Compared with the accurate buckling load from the DLU method, the FPD buckling theory is able to give a better prediction, while the CBT and CNM may yield unacceptable results (with 70% error for the buckling of an elastic semi-plane solid).

Finally, it is significant to further discuss the applicability of the FPD buckling theory. When the prebuckling deformation becomes non-negligible, the CBT and the CNM may yield an unacceptable error for the critical buckling load, while our FPD buckling theory is able to give a better result. For example, the CBT yields more than 40% error compared with the accurate solution for the buckling of an elastic rectangular solid with aspect ratio of L: $2t = 5{:}1$, while the results obtained by the FPD buckling theory is much better. For larger aspect ratio L: $2t$, the difference between the CBT, CNM, FPD, and DLU becomes smaller. Therefore, the criterion of L: $2t < 5{:}1$ for the elastic rectangular solid is suggested for considering the effect of the prebuckling deformation. Usually, the FPD buckling theory is significant to the analysis of the soft materials, flexible, and stretchable structures such as human skin, soft robots, and compliant substrate for flexible electronics. In the future work, the FPD buckling theory will apply to the film-substrate structure that has attracted much attention.

Acknowledgment

Y. S. gratefully acknowledges the support from the National Natural Science Foundation of China (No. 12172359, 11772331, 11572323; Funder ID: 10.13039/501100001809), Beijing Municipal Science and Technology Commission (No. Z191100 002019010; Funder ID: 10.13039/501100009592), Beijing Municipal Natural Science Foundation (No. 2202066; Funder ID: 10.13039/501100004826), Key Research Program of Frontier Sciences of the Chinese Academy of Sciences (No. ZDBS-LY-JSC014), CAS Interdisciplinary Innovation Team (No. JCTD-2020-03), Strategic Priority Research Program of the Chinese Academy of Sciences (No. XDB22040501), and the State Key Laboratory of Structural Analysis for Industrial Equipment, Dalian University of Technology (No. GZ19102; Funder ID: 10.13039/501100002980).

Author Contributions

Y. S. found the class of structures and developed the framework of the theory. Y. S. and H. Z. derived the theory, performed the numerical simulation, and wrote the manuscript.

Conflict of Interest

There are no conflicts of interest.

Data Availability Statement

The authors attest that all data for this study are included in the paper.

Appendix A: Conventional Numerical Method (CNM) for Critical Buckling

The finite element method for critical buckling in commercial program package ABAQUS [46] is based on the CBT, with the consideration of the prebuckling stress/force but without considering prebuckling deformation. The numerical solver for critical

buckling loads and buckling modes of structures is *general/linear perturbation* in ABAQUS CAE/input file. It is also called the solver for linear buckling. It results in a linear eigenvalue problem in mathematics.

Appendix B: Buckling Analysis of an Elastic Semi-Plane Solid by Ogden's Theory

To compare the FPD buckling theory and the work given by Ogden, Ogden's theory [26] is applied to the buckling of an elastic semi-plane solid with the Saint-Venant-Kirchhoff constitutive model. The equilibrium equation described in the reference state is

$$\mathrm{Div}\boldsymbol{S} = 0 \tag{B1}$$

where $\boldsymbol{S}$ is the first Piola-Kirchhoff stress. The constitutive model is expressed as

$$\boldsymbol{S} = \boldsymbol{\Lambda F} \tag{B2}$$

where $\boldsymbol{\Lambda}$ is the instantaneous elastic moduli, which, in component form, is given by

$$\Lambda_{AiBj} = L_{AkBl}F_{ik}F_{jl} + T_{AB}\delta_{ij} \tag{B3}$$

Here, L_{AkBl} is the component of the elastic tensor $\boldsymbol{L}$, which is same with it in the Saint-Venant-Kirchhoff model, F_{ik} the component of the deformation gradient $\boldsymbol{F}$, T_{AB} the component of the second type of P-K stress, respectively.

The equilibrium equation for the critical buckling behaviors is

$$\mathrm{Div}\Delta\boldsymbol{S} = 0 \tag{B4}$$

and the component of the first Piola-Kirchhoff stress is

$$\Delta S_{iA} = \Lambda_{AiBj}\Delta U_{j,B} \tag{B5}$$

where ΔU denotes the incremental displacement. The constitutive equation becomes

$$\Lambda_{AiBj} = L_{AkBl}\overset{\circ}{F}_{ik}\overset{\circ}{F}_{jl} + \overset{\circ}{T}_{AB}\delta_{ij} \tag{B6}$$

From the brebuckling analysis, we can obtain $\overset{\circ}{F}_{11} = 1-\alpha$, $\overset{\circ}{F}_{12} = \overset{\circ}{F}_{21} = 0$, $\overset{\circ}{F}_{22} = 1+\nu\alpha$, and $\overset{\circ}{T}_{11} = \alpha\bar{E}$. Equation (B6) gives the components of the instantaneous elastic moduli

$$\begin{aligned}
&\Lambda_{1111} = (\lambda-2\mu)(1-\underline{\alpha})^2 - \alpha\bar{E}\\
&\Lambda_{1122} = \Lambda_{2211} = \lambda(1-\underline{\alpha})(1+\underline{\nu\alpha})\\
&\Lambda_{2121} = \mu(1-\underline{\alpha})^2\\
&\Lambda_{1212} = \mu(1+\underline{\nu\alpha})^2 - \alpha\bar{E}\\
&\Lambda_{1221} = \Lambda_{2112} = \mu(1+\underline{\nu\alpha})(1-\underline{\alpha})\\
&\Lambda_{2222} = (\lambda-2\mu)(1+\underline{\nu\alpha})^2
\end{aligned} \tag{B7}$$

The underlined terms in the above and following equations are for the effect of the prebuckling deformation. Substitution of Eq. (B7) into Eq. (B5) gives the components of the first Piola-Kirchhoff stress:

$$\begin{aligned}
\Delta S_{11} &= \left[\frac{\overline{E}}{1-\bar{\nu}^2}(1-\underline{\alpha})^2 - \alpha\bar{E}\right]\frac{\partial\Delta U_1}{\partial X_1} + \frac{\bar{\nu}\overline{E}}{1-\bar{\nu}^2}(1-\underline{\alpha})(1+\underline{\bar{\nu}\alpha})\frac{\partial\Delta U_2}{\partial X_2}\\
\Delta S_{12} &= \frac{\overline{E}}{2(1+\bar{\nu})}(1-\underline{\alpha})^2\frac{\partial\Delta U_1}{\partial X_2} + \frac{\overline{E}}{2(1+\bar{\nu})}(1+\underline{\bar{\nu}\alpha})(1-\underline{\alpha})\frac{\partial\Delta U_2}{\partial X_1}\\
\Delta S_{21} &= \left[\frac{\overline{E}}{2(1+\bar{\nu})}(1+\underline{\bar{\nu}\alpha})^2 - \alpha\bar{E}\right]\frac{\partial\Delta U_2}{\partial X_1} + \frac{\overline{E}}{2(1+\bar{\nu})}(1+\underline{\bar{\nu}\alpha})(1-\underline{\alpha})\frac{\partial\Delta U_1}{\partial X_2}\\
\Delta S_{22} &= \frac{\bar{\nu}\overline{E}}{1-\bar{\nu}^2}(1-\underline{\alpha})(1+\underline{\bar{\nu}\alpha})\frac{\partial\Delta U_1}{\partial X_1} + \frac{\overline{E}}{1-\bar{\nu}^2}(1+\underline{\bar{\nu}\alpha})^2\frac{\partial\Delta U_2}{\partial X_2}
\end{aligned} \tag{B8}$$

The combination of Eqs. (B4) and (B8) yields the equilibrium equations in terms of the displacements

$$\begin{aligned}
&[(1-\underline{\alpha})^2 - \alpha(1-\bar{\nu}^2)]\frac{\partial^2\Delta U_1}{\partial X_1^2} + \frac{1-\bar{\nu}}{2}(1-\underline{\alpha})^2\frac{\partial^2\Delta U_1}{\partial X_2^2} + \frac{1+\bar{\nu}}{2}(1-\underline{\alpha})(1+\underline{\bar{\nu}\alpha})\frac{\partial^2\Delta U_2}{\partial X_1\partial X_2} + \frac{\partial^2\Delta U_1}{\partial X_1^2} = 0\\
&\left[\frac{1-\bar{\nu}}{2}(1+\underline{\bar{\nu}\alpha})^2 - \alpha(1-\bar{\nu}^2)\right]\frac{\partial^2\Delta U_2}{\partial X_1^2} + (1+\underline{\bar{\nu}\alpha})^2\frac{\partial^2\Delta U_2}{\partial X_2^2} + \frac{1+\bar{\nu}}{2}(1+\underline{\bar{\nu}\alpha})(1-\underline{\alpha})\frac{\partial^2\Delta U_1}{\partial X_1\partial X_2} = 0
\end{aligned} \tag{B9}$$

The traction-free boundary condition is

$$\boldsymbol{\sigma}\cdot d\boldsymbol{a} = \boldsymbol{S}\cdot d\boldsymbol{A} = 0 \tag{B10}$$

which yields

$$\begin{aligned}
&(1-\underline{\alpha})^2\frac{\partial\Delta U_1}{\partial X_2} + (1+\underline{\bar{\nu}\alpha})(1-\underline{\alpha})\frac{\partial\Delta U_2}{\partial X_1} = 0\\
&(1+\underline{\bar{\nu}\alpha})^2\frac{\partial\Delta U_2}{\partial X_2} + \bar{\nu}(1-\underline{\alpha})(1+\underline{\bar{\nu}\alpha})\frac{\partial\Delta U_1}{\partial X_1} = 0
\end{aligned}, \quad \text{at } X_2 = 0 \tag{B11}$$

References

[1] Euler, L., 1744, *Methodus Inveniendi Lineas Curvas Maximi Minimive Proprietate Gaudentes*, Apud Marcum-Michaelem Bousquet.

[2] Lagrange, J. L., Serret, J. A., and Darboux, G., 1867, *Oeuvres de Lagrange*, Gauthier-Villars, Paris.

[3] Kim, D. H., Song, J., Choi, W. M., Kim, H. S., Kim, R. H., Liu, Z., Huang, Y. Y., Hwang, K. C., Zhang, Y. W., and Rogers, J. A., 2008, "Materials and Noncoplanar Mesh Designs for Integrated Circuits With Linear Elastic Responses to Extreme Mechanical Deformations," Proc. Natl. Acad. Sci. U. S. A., **105**(48), pp. 18675–18680.

[4] Su, Y., Wu, J., Fan, Z., Hwang, K., Song, J., Huang, Y., and Rogers, J. A., 2012, "Postbuckling Analysis and Its Application to Stretchable Electronics," J. Mech. Phys. Solids, **60**(3), pp. 487–508.

[5] Jiang, H., Khang, D. Y., Song, J., Sun, Y., Huang, Y., and Rogers, J. A., 2007, "Finite Deformation Mechanics in Buckled Thin Films on Compliant Supports," Proc. Natl. Acad. Sci. U. S. A., **104**(40), pp. 15607–15612.

[6] Fan, Z., Hwang, K. C., Rogers, J. A., Huang, Y., and Zhang, Y., 2018, "A Double Perturbation Method of Postbuckling Analysis in 2D Curved Beams for Assembly of 3D Ribbon-Shaped Structures," J. Mech. Phys. Solids, **111**, pp. 215–238.

[7] Timoshenko, S. P., and Gere, J. M., 1961, *Theory of Elastic Stability*, 2nd ed., McGraw-Hill, New York.

[8] Khang, D., Jiang, H., Huang, Y., and Rogers, J. A., 2006, "A Stretchable Form of Single-Crystal Silicon for High-Performance Electronics on Rubber Substrates," Science, **311**(5758), pp. 208–212.
[9] Fu, Y. B., and Ogden, R. W., 1999, "Nonlinear Stability Analysis of Pre-Stressed Elastic Bodies," Continuum Mech. Thermodyn., **11**(3), pp. 141–172.
[10] Fu, Y., and Rogerson, G. A., 1994, "A Nonlinear Analysis of Instability of a Pre-Stressed Incompressible Elastic Plate," Proc. R. Soc. London, A, **446**(1927), pp. 233–254.
[11] Chadwick, P., and Ogden, R., 1971, "On the Definition of Elastic Moduli," Arch. Ration. Mech. Anal., **44**(1), pp. 41–53.
[12] Su, Y., Ping, X., Yu, K. J., Lee, J. W., Fan, J. A., Wang, B., Li, M., et al., 2017, "In-Plane Deformation Mechanics for Highly Stretchable Electronics," Adv. Mater., **29**(8), p. 1604989.
[13] Su, Y., Zhao, H., Liu, S., Li, R., Wang, Y., Wang, Y., Bian, J., and Huang, Y., 2019, "Buckling of Beams With Finite Prebuckling Deformation," Int. J. Solids Struct., **165**(15), pp. 148–159.
[14] Biot, M. A., 1938, "Theory of Elasticity With Large Displacements and Rotations," Proceedings of the Fifth International Congress of Applied Mechanics, pp. 117–122.
[15] Biot, M. A., 1959, "Folding of a Layered Viscoelastic Medium Derived From an Exact Stability Theory of a Continuum Under Initial Stress," Q. Appl. Math., **17**(2), pp. 185–204.
[16] Biot, M. A., 1963, "Surface Instability of Rubber in Compression," Appl. Sci. Res., **12**(2), pp. 168–182.
[17] Biot, M. A., and Romain, J. E., 1965, "Mechanics of Incremental Deformations," J. Appl. Mech., **32**(4), p. 957.
[18] Novozhilov, V. V., 1953, *Foundations of the Nonlinear Theory of Elasticity*, Graylock Press, New York.
[19] Kerr, A. D., and Tang, S., 1967, "The Instability of a Rectangular Elastic Solid," Acta Mechanica, **4**(1), pp. 43–63.
[20] Brunelle, E. J., 1973, "Surface Instability Due to Initial Compressive Stress," Bull. Seismol. Soc. Am., **63**(6-1), pp. 1885–1893.
[21] Triantafyllidis, N., 1983, "On the Bifurcation and Postbifurcation Analysis of Elastic-Plastic Solids Under General Prebifurcation Conditions," J. Mech. Phys. Solids, **31**(6), pp. 499–510.
[22] Jiménez, F. L., and Triantafyllidis, N., 2013, "Buckling of Rectangular and Hexagonal Honeycomb Under Combined Axial Compression and Transverse Shear," Int. J. Solids Struct., **50**(24), pp. 3934–3946.
[23] Triantafyllidis, N., 1980, "Bifurcation Phenomena in Pure Bending," J. Mech. Phys. Solids, **28**(3), pp. 221–245.
[24] Lee, D., Triantafyllidis, N., Barber, J. R., and Thouless, M. D., 2008, "Surface Instability of an Elastic Half Space With Material Properties Varying With Depth," J. Mech. Phys. Solids, **56**(3), pp. 858–868.
[25] Ogden, R., and Fu, Y., 1996, "Nonlinear Stability Analysis of a Pre-Stressed Elastic Half-Space," Contemp. Res. Mech. Math. Mater., pp. 164–175.
[26] Ogden, R. W., 1984, *Non-Linear Elastic Deformations*, Dover Publications, Inc., New York.
[27] Bažant, Z., 1971, "A Correlation Study of Formulations of Incremental Deformation and Stability of Continuous Bodies," ASME J. Appl. Mech., **38**(4), pp. 919–928.
[28] Goodier, J. N., and Plass, H. J., 1952, "Energy Theorems and Critical Load Approximations in the General Theory of Elastic Stability," Q. Appl. Math., **9**(4), pp. 286–287.
[29] Eringen, A., and Paslay, P. R., 1964, "Non-Linear Theory of Continuous Media," ASME J. Appl. Mech., **31**(4), p. 368.
[30] Huang, Z. Y., Hong, W., and Suo, Z., 2005, "Nonlinear Analyses of Wrinkles in a Film Bonded to a Compliant Substrate," J. Mech. Phys. Solids, **53**(9), pp. 2101–2118.
[31] Huang, R., 2005, "Kinetic Wrinkling of an Elastic Film on a Viscoelastic Substrate," J. Mech. Phys. Solids, **53**(1), pp. 63–89.
[32] Chen, X., and Hutchinson, J. W., 2004, "Herringbone Buckling Patterns of Compressed Thin Films on Compliant Substrates," ASME J. Appl. Mech., **71**(5), pp. 597–603.
[33] Bowden, N., Brittain, S., Evans, A., Hutchinson, J., and Whitesides, G., 1998, "Spontaneous Formation of Ordered Structures in Thin Films of Metals Supported on an Elastomeric Polymer," Nature, **393**(6681), pp. 146–149.
[34] Song, J., Jiang, H., Liu, Z. J., Khang, D. Y., Huang, Y., Rogers, J. A., Lu, C., and Koh, C., 2008, "Buckling of a Stiff Thin Film on a Compliant Substrate in Large Deformation," Int. J. Solids Struct., **45**(10), pp. 3107–3121.
[35] Jiang, H., Khang, D., Fei, H., Kim, H., Huang, Y., Xiao, J., and Rogers, J. A., 2008, "Finite Width Effect of Thin-Films Buckling on Compliant Substrate: Experimental and Theoretical Studies," J. Mech. Phys. Solids, **56**(8), pp. 2585–2598.
[36] Bo, L., Huang, S. Q., and Feng, X. Q., 2010, "Buckling and Postbuckling of a Compressed Thin Film Bonded on a Soft Elastic Layer: A Three-Dimensional Analysis," Arch. Appl. Mech., **80**(2), p. 175.
[37] Li, B., Zhao, H., and Feng, X., 2011, "Spontaneous Instability of Soft Thin Films on Curved Substrates Due to van der Waals Interaction," J. Mech. Phys. Solids, **59**(3), pp. 610–624.
[38] Li, B., Cao, Y., Feng, X.-Q., and Gao, H., 2012, "Mechanics of Morphological Instabilities and Surface Wrinkling in Soft Materials: A Review," Soft Matter, **8**(21), pp. 5728–5745.
[39] Holland, M. A., Li, B., Feng, X. Q., and Kuhl, E., 2017, "Instabilities of Soft Films on Compliant Substrates," J. Mech. Phys. Solids, **98**, pp. 350–365.
[40] Huang, S., and Li, B., 2008, "Three-Dimensional Analysis of Spontaneous Surface Instability and Pattern Formation of Thin Soft Films," J. Appl. Phys., **103**(8), p. 545.
[41] Wang, P., Casadei, F., Shan, S., Weaver, J. C., and Bertoldi, K., 2014, "Harnessing Buckling to Design Tunable Locally Resonant Acoustic Metamaterials," Phys. Rev. Lett., **113**(1), p. 014301.
[42] Bertoldi, K., Reis, P. M., Willshaw, S., and Mullin, T. J. A. M., 2010, "Negative Poisson's Ratio Behavior Induced by an Elastic Instability," Adv. Mater., **22**(3), pp. 361–366.
[43] Bertoldi, K., Boyce, M. C., Deschanel, S., Prange, S. M., and Mullin, T., 2008, "Mechanics of Deformation-Triggered Pattern Transformations and Superelastic Behavior in Periodic Elastomeric Structures," J. Mech. Phys. Solids, **56**(8), pp. 2642–2668.
[44] Biot, M. A., 1965, *Mechanics of Incremental Deformations*, John Wiley and Sons Inc., New York.
[45] Cao, Y., and Hutchinson, J. W., 2012, "From Wrinkles to Creases in Elastomers: The Instability and Imperfection-Sensitivity of Wrinkling," Proc. R. Soc. A, **468**(2137), pp. 94–115.
[46] Dassault-Systèmes, 2010, *Abaqus Analysis User's Manual v.6.10*, Dassault Systèmes Simulia Corp., Johnston, RI.